ORNL/TM-11608

ornl

OAK RIDGE
NATIONAL
LABORATORY

MARTIN MARIETTA

Loss Analysis of the Thermodynamic Cycle of Magnetic Heat Pumps

Phase I Final Report of Thermal Sciences Research Program on Thermophysics of Magnetocaloric Energy Conversion

F. C. Chen
R. W. Murphy
V. C. Mei
G. L. Chen
J. W. Lue
M. S. Lubell

MANAGED BY
MARTIN MARIETTA ENERGY SYSTEMS, INC.
FOR THE UNITED STATES
DEPARTMENT OF ENERGY

This report has been reproduced directly from the best available copy.

Available to DOE and DOE contractors from the Office of Scientific and Technical Information, P.O. Box 62, Oak Ridge, TN 37831; prices available from (615) 576-8401, FTS 626-8401.

Available to the public from the National Technical Information Service, U.S. Department of Commerce, 5285 Port Royal Rd., Springfield, VA 22161.

This report was prepared as an account of work sponsored by an agency of the United States Government. Neither the United States Government nor any agency thereof, nor any of their employees, makes any warranty, express or implied, or assumes any legal liability or responsibility for the accuracy, completeness, or usefulness of any information, apparatus, product, or process disclosed, or represents that its use would not infringe privately owned rights. Reference herein to any specific commercial product, process, or service by trade name, trademark, manufacturer, or otherwise, does not necessarily constitute or imply its endorsement, recommendation, or favoring by the United States Government or any agency thereof. The views and opinions of authors expressed herein do not necessarily state or reflect those of the United States Government or any agency thereof.

ORNL/TM-11608

LOSS ANALYSIS OF THE THERMODYNAMIC CYCLE OF MAGNETIC HEAT PUMPS

Phase I Final Report
of
Thermal Sciences Research Program
on
Thermophysics of Magnetocaloric Energy Conversion

F. C. Chen,* R. W. Murphy,* V. C. Mei,* G. L. Chen,†
J. W. Lue,‡ and M. S. Lubell‡

DATE PUBLISHED: February 1991

Prepared for
ADVANCED INDUSTRIAL CONCEPTS DIVISION
OFFICE OF INDUSTRIAL TECHNOLOGIES

by the
OAK RIDGE NATIONAL LABORATORY
Oak Ridge, Tennessee 37831-6285
managed by
MARTIN MARIETTA ENERGY SYSTEMS, INC.
for the
U. S. DEPARTMENT OF ENERGY
under Contract Number DE-AC05-84OR21400

* Energy Division
† Computer Science & Telecommunications Division
‡ Fusion Energy Division

TABLE OF CONTENTS

ABSTRACT v

1. INTRODUCTION 1

2. LITERATURE SURVEY 3
   2.1 SCOPE OF THE REVIEW 3
   2.2 THEORIES 3
   2.3 MATERIALS AND PROPERTIES 4
   2.4 OPERATING CYCLES 5
   2.5 EXPERIMENTAL DATA 6
   2.6 SYSTEM CONCEPTS 6
   2.7 "GENERIC" PUBLICATIONS 6
   2.8 THE ENTROPY OF GADOLINIUM 6

3. MAGNETOCALORIC CYCLE ANALYSIS 11
   3.1 BASIC CYCLES 11
      3.1.1 Boundary work cycles 12
      3.1.2 Magnetic work cycles 14
   3.2 MAGNETOCALORIC MATERIAL MODELING 15
      3.2.1 Comparison with existing data 16
   3.3 CYCLE MODELING 16
      3.3.1 Carnot cycle 16
      3.3.2 Constant magnetization cycle 17
      3.3.3 Ideal regenerative cycle 18
      3.3.4 Constant-field cycle 19

4. CYCLE ENERGY LOSSES 21
   4.1 MODEL OF HEAT TRANSFER BETWEEN MAGNETIC MATERIALS AND REGENERATOR FLUID 21
   4.2 HEAT LOSSES 23
      4.2.1 Eddy current loss 23
      4.2.2 Magnetic hysteresis loss 24
      4.2.3 Demagnetization field 24
      4.2.4 Magnetic force induced by external field on the gadolinium core 25

5. PULSED DC MAGNET ANALYSIS 27
   5.1 PULSE MAGNET DESIGN 27
   5.2 AC LOSS ANALYSIS 28
   5.3 TANDEM SYSTEM CONSIDERATION 29

6. CONCLUSIONS AND RECOMMENDATIONS 31

REFERENCES 33

FIGURES 37

APPENDIX A: Computer Code for Analysis of Heat Pump Cycles 57

APPENDIX B: Example of Loss Calculations 61

APPENDIX C: Transient Heat Transfer Model for a Magnetic Heat Pump 64

ABSTRACT

Recently, the needs for developing non–ozone-depleting, no–greenhouse-effect heat pump systems and for exploring the potential of new high-temperature superconducting materials have prompted a renewed interest in the study of magnetic heat pumps. The new materials can provide the high magnetic field that an effective superconducting magnetic heat pump requires, and magnetic heat pumps do not use freon for a working fluid. Traditionally, magnetic heat pump concepts have been successfully developed and used for refrigeration applications at temperatures near absolute zero degree. In these cases, a temperature lift of a few degrees in a cryogenic environment is sufficient and can be easily achieved by a simple magnetic heat pump cycle. The working media are usually the chemical compounds of gadolinium. To extend magnetic heat pumping to other temperature ranges and other types of applications in which the temperature lift is more than just a few degrees requires more involved cycle processes dependent upon the thermomagnetic properties of the working media and the availability of a high magnetic field. This report documents our efforts to study the thermophysics of magnetic heat pumps, including a survey of literature, a study of thermodynamic cycles and cycle thermal losses, and an analysis of pulse magnets. The regenerative cycle has been identified as the most efficient, with a maximum of 42% loss in coefficient of performance at 260 K cooling temperature and a maximum of 15% loss in capacity at 232 K cooling temperature for the constant field (magnetic Ericsson) cycle, between 200 K and 320 K, as compared with the ideal regenerative cycle with gadolinium as the core material.

1. INTRODUCTION

The concept of the magnetic heat pump is based on the principle of magnetocaloric effect of magnetic materials, in which entropy, and therefore temperature, changes when a material is magnetized or demagnetized. When a soft magnetic material is in its natural (i.e., zero magnetic field) state, the magnetic dipoles in the material are in a relatively disordered state; if a magnetic field is imposed upon the material, the dipoles align with the field and are transformed into an ordered state, and a decrease in entropy (corresponding to an increase in temperature) occurs. Conversely, if a magnetic material is suddenly demagnetized by being removed from a magnetic field, an increase in entropy and a corresponding decrease in temperature will occur.

The origin of the concept of magnetic cooling can be traced back more than a half century to the 1920s, when Giauque [1] and Debye [2] independently proposed using the magnetocaloric effect of magnetic materials for refrigeration to produce ultra-low temperatures. In 1933, Giauque was able to achieve a cooling temperature of 0.5 K down from 3.5 K by using the magnetocaloric effect [3]. His method was to cool a paramagnetic salt to 3.5 K in a magnetic field and then to demagnetize it adiabatically to achieve 0.5 K. This adiabatic demagnetization method is a one-shot or single-step refrigeration process that does not provide continuous cooling. It is still being used in low-temperature physics experiments to create temperatures extremely close to absolute zero.

The possibility of building a heat pump using the magnetocaloric effect was apparently first suggested in 1949 by Daunt [4], who combined two isothermal and two adiabatic magnetization and demagnetization processes to form a magnetic Carnot heat pump cycle that is capable of providing the sustained cooling. However, the laboratory experimentation was not performed until 1975, when Brown built and tested a reciprocating magnetic heat pump assembly using gadolinium as the working medium [5] . Brown's study of magnetic heat pumps was aimed primarily toward near-room-temperature space-conditioning applications. Since then, many experimental and analytical studies have been done on the heat pump concept, and the end-use applications vary from 4 K in the liquid-helium temperature range, such as the study of magnetic refrigerators by Barclay [6], to 400 K, such as in the production of low-pressure steam for industrial heating by the Idaho National Engineering Laboratory [7].

Like the magnetic properties of materials, the temperature change caused by the magnetocaloric effect is highly dependent upon a strong magnetic field. Strong fields created by superconducting magnets are often preferred and are probably necessary for many practical applications. The complexity and relatively high cost of traditional superconducting magnets (which

must be cooled by liquid He) are among the factors that have affected interest in magnetic heat pump development. The discovery of high-temperature superconductivity shows promise for achieving not only higher magnetic fields than before but also for being a simpler and less costly option (which may be cooled by liquid N_2). Continued advancement in new superconducting materials research will enhance the viability of magnetic heat pump technology as well. In view of the recent rapid progress in the superconductivity area, we have investigated many possible options for magnetic heat pump concepts that could utilize the newly discovered materials and technology. A test rig for a superconducting magnetic heat pump was assembled using an existing low-temperature superconducting magnet. This was an internally supported effort by the ORNL Exploratory Studies Program. Noticeable temperature lift was achieved. However, the existing magnet is not designed for the pulse-DC mode of operation needed in the test setup. Sustained experimentation of regenerative magnetic heat pumping was not fulfilled in the initial internal R&D study.

This report documents our study, with DOE sponsorship, of the thermophysics of magnetic heat pumps, which includes a survey of literature, a study of thermodynamic cycles and cycle thermal losses, and an analysis of pulse magnets. The temperature lift that can be achieved by a magnetic Carnot cycle is limited by the obtainable strength of the magnetic field. Temperature lifts beyond those that can be attained by a magnetic Carnot cycle will have to be done by other cycle processes. Three magnetic cycles capable of higher temperature lifts were analyzed. We found that the ideal regenerative cycle is the most efficient one studied, and that the performances and capacities of other cycles could be increased substantially in certain operating-temperature ranges. Several cycle thermal losses (identified in previous studies [6, 8] but not analyzed) were examined. Estimated power losses of a pulse-magnet design to be used in a mechanically static magnetic heat pump were also investigated.

2. LITERATURE SURVEY

V. C. Mei

2.1 SCOPE OF THE REVIEW

A literature search was performed. Communication with people in this field through personal contacts provided valuable up-to-date information.

Earlier work, that done before 1976, mostly involved the application of the magnetocaloric effect in the cryogenics field with temperatures close to absolute zero. It is only recently that magnetic heat pumps (MHPs) have been considered for applications with a temperature range from 20 K to near room temperature [1], such as hydrogen liquefaction, cooling of high-temperature superconducting devices, cooling of industrial chemical processes, industrial and domestic refrigeration, and air-conditioning. This effort concentrates on publications in this temperature range, and thus eliminates most of the publications because magnetic heat pumps are traditionally used in the low-temperature cryogenics field.

The current review is divided into several categories including literature dealing with

- theories about the MHP,
- magnetocaloric materials and their properties,
- operating cycles,
- existing experimental data, and
- system concepts.

The cost and availability of some of the commercially available materials used above 273 K are discussed in detail in reference [2].

2.2 THEORIES

MHPs are an application of the "magnetocaloric effect" that some materials have in a magnetic field. Reference [1] provides a good summary of MHP theories. The magnetic moment and its interaction with thermal and mechanical properties are basically adding the term "magnetic work" to the internal energy equation [1, 3–6]. The entropy change associated with temperature and magnetic field can be considered in three respects: lattice entropy, electronic entropy, and magnetic entropy [7–9].

- Lattice entropy: the entropy associated with the vibration of the molecules, which is also a function of temperature. It is complicated to calculate because it involves the application of Debye temperature (which is a material property) and Debye function [7–9].
- Electronic entropy: the kinetic entropy of the electrons. It is a function of temperature.
- Magnetic entropy: the entropy change caused by the spin of the molecules when the material is magnetized under the magnetic field. It involves the strength of the magnetic field, material properties, temperatures, Curie point, and the application of Brillouin function [10, 11].

To calculate the performance of an MHP system, all three entropy components must be considered. Besides, many heat transfer problems are involved in actual MHP systems. Reference [3] describes in detail two heat transfer models of a regenerative magnetic refrigerator. With some modification, these models can be used to calculate the performance of regenerative MHPs [12]. Some of the losses of MHP systems were discussed in reference [13].

2.3 MATERIALS AND PROPERTIES

Whether a material is suitable for MHP application depends on its "magnetocaloric effect" around the Curie point. The following list shows materials that have been used or considered for the MHP for the above-mentioned temperature range.

Material	Curie Temperature (K)	Reference
Dysprosium (Dy)	17	[21]
$ErAl_2$	22	[8]
$HoAl_2$	42	[8]
$DyAl_{2.2}$	51	[14]
Thulium (Tm)	55	[15]
$DyAl_2$	70	[8]
Ho_5Si_4	76	[8]
Erbium (Er)	83	[16, 17]
Europium (Eu)	88.8	[18]
Holmium (Ho)	131	[19, 20]
Terbium (Tb)	230	[19, 22]

Materials to be used above 273 K are:

Material	Curie Temperature (K)	Reference
Gd_5Si_4	336	[8]
Gadolinium (Gd)	291	[23]
Gd_3Al_2	282	[8]

Many other materials are available that have Curie points in the temperature range of interest. Reference [9] lists some materials that can be used above 300 K. Of those materials, however, only Gd has been well studied. Information for others is very rare. There might be other material problems. For example, Tb is an anisotropic material for which the tests are still ongoing [24]. Some experimental results indicated that it is possible to control the Curie points of complex magnetic materials using the ferromagnetic material series [25]. Reference [26] shows the Curie points of R-Y (rare earth metal and yttrium) alloys as a function of alloy material composition. References [8] and [27–30] show a variety of examples of some pure ferromagnetic rare-earth elements and alloys whose Curie points vary from 24 K to near room temperature. Some materials, such as chromium and manganese, are considered strategic materials. Use of a large quantity of such materials may interfere with government policy [31].

The thermophysical properties of some of the just-discussed materials are listed in reference [32]. However, we are still searching for information for some of the materials. Nigh et al. measured the magnetization and electrical resistivity of gadolinium single crystals [33]. Appendix A provides some of the thermophysical properties of gadolinium as an example. References [34–37] provide useful information on the material properties and application of complex magnetic materials in the temperature range of 20 K to 77 K.

2.4 OPERATING CYCLES

Most magnetic heat pumps operated on the Ericsson cycle between two constant magnetic fields, or with one constant field and one variable but controlled field [14, 38]. Theoretically, an Ericsson cycle with perfect regeneration will have the same efficiency as the Carnot cycle, but with a much-extended operating temperature range [39]. The Brayton cycle was discussed in references [13] and [39]. Other cycles such as the recuperative cycle and the recuperative Brayton cycle were also discussed in reference [39].

2.5 EXPERIMENTAL DATA

The heat capacities of some of the materials used for MHPs in cryogenic applications have been experimentally measured [15–23]. For MHP systems near room temperature, information on heat capacities is limited. Brown and Papell [40] tested a regenerative MHP with Gd as the core material and with an ethanol and water mixture as the regenerative fluid. The system, under no load condition, managed to have an 80-K temperature differential between cold and warm ends of the fluid after 50 cycles. However, steady-state operation was not achieved. Experimental data on magnetic refrigeration for the temperature range of 20–77 K is also limited. One paper reported the test of an experimental unit which used a composite of several sintered aluminum compounds of rare-earth metal as the working magnetic material [41].

2.6 SYSTEM CONCEPTS

In the many feasibility studies, several design concepts were discussed [4, 13, 38]. Brown provided several Gd core design concepts [38]. Kirol et al. discussed in detail a baseline reciprocal machine and counterflow rotary MHP design concept [13]. Hull and Uherka discussed the magnetic field switching concept [42], which has the advantage of having the least amount of mechanical motion. This design [42] can transfer the magnetic energy from one inductor to another or from one inductor to and from the power grid, or a combination of both.

2.7 "GENERIC" PUBLICATIONS

Some publications of general interest in this field that do not fit the above description are also collected in the references, such as those on the numerical model [43, 44], that on theory for a ferromagnetic heat engine with a ferromagnetic wheel [45], that on a bench scale for a rotary recuperative magnetic heat pump [46], that on preparation and fabrication of rare earth magnetic materials [47], and that on recent developments in cryogenic coolers [48].

2.8 THE ENTROPY OF GADOLINIUM

In order to analyze MHP cycles, one needs to know the entropy change produced in a magnetic material when it is subjected to changes in external magnetic field and temperature. Solids,

particularly metals, consist of many particles that interact with each other appreciably by means of ion spins, lattice vibrations, and conduction electron flow. When the system is perturbed by an external magnetic field or by temperature, the entropy will be changed accordingly. Among these three interactions, the conduction electron flow is the weakest. The lattice vibration interaction can be neglected at low temperatures. However, at higher temperatures, the lattice vibrations and conduction electron interactions may be very strong. For a magnetic heat pump to be operated near room temperature, all three interactions must be considered. Previous work provided a theoretical foundation for computing the entropy of gadolinium.

Since the second law of thermodynamics allows us to write C dT = T dS, the entropy can be calculated in terms of heat capacity (C), if heat capacity is known,

$$S-S_o=\int_{T_o}^{T}\frac{C}{T}\,dT\,. \tag{2-1}$$

In general, heat capacity can be measured experimentally. The heat capacity of Gd from 15 to 355 K at zero field was measured by Griffel et al. [49]. This experimental data was widely used to calculate Gd entropy [23]. In this paper, we have theoretically calculated Gd entropy and then compared it with the experimental data.

We begin with the spin interaction by considering a solid consisting of many identical atoms arranged in a regular lattice. Each atom has a net electron spin and associated magnetic moment. In the presence of an externally applied magnetic field, the interaction of the atoms with this field and neighboring atoms will produce the magnetic entropy that is given by the following expression, according to Weiss' molecular-field approximation [50],

$$S_M=R\,\{\,\ln[\sinh(2J+1)x/2J]/[\sinh(x/2J)]-xB_J(x)\,\} \tag{2-2}$$

where R is the universal gas constant and J is the resultant of orbital and spin quantum numbers.

$$x=\mu_B gJ(H+K_W M)/kT\,, \tag{2-3}$$

$$M=Ng\mu_B JB_J(x)\,,\ and \tag{2-4}$$

$$B_J=\{\,(J+1/2)\coth[(J+1/2)x]-1/2\coth(x/2)\,\}\,, \tag{2-5}$$

where

M is the magnetization,

μ_B is the Bohr magneton,

g is the Lande splitting factor,

N is the number of dipoles,

H is the external magnetic field,

K_W is a constant called the molecular field constant,

k is the Boltzmann constant,

T is temperature.

B_J is called the Brillouin function. For Gd, g=2 and J=7/2.

The Gd magnetic (spin) entropy is shown in Fig. 2.1 as a function of H and T. The normalized magnetization (M/M_0) is shown is Fig. 2.1 as well, where $M_0=Ng\mu_B J$. Fig. 2.1 shows that the Gd entropy increases as temperature increases, but decreases as the strength of the magnetic field increases. There is also a sharp cusp near the Curie point (291 K) at zero field. If a higher order of spin interaction is included in the Weiss theory, this cusp might be smoothed out somewhat, but the work is beyond this study. Brown [11] applied Weiss' theory to calculate Gd entropy.

Next, we consider the lattice vibration interaction by using the Debye approximation [51]. The lattice heat capacity is given by the following expression.

$$C_L = 9Nk\left(\frac{T}{\theta_D}\right)^3 \int_o^{\frac{\theta_D}{T}} \frac{e^y}{(e^y-1)^2} y^4 dy \ , \tag{2-6}$$

where Θ is defined as the Debye temperature, which is 172 K for Gd [3]. The lattice entropy can be expressed as follows.

$$S_L = 9NK\int_O^T \left(\frac{T}{\Theta_D}\right)^3 dT \int_O^{\frac{\Theta_D}{T}} \frac{e^y}{(e^y-1)^2} y^4 dy \tag{2-7}$$

Because of the involvement of singularities, the numerical evaluation of Eq. 2-7 becomes difficult. However, Eq. 2-7 can be simplified by integration by parts to the form as follows.

$$S_L = R\left[-3\ln\left(1-e^{\frac{-\theta_D}{T}}\right)+12\left(\frac{T}{\theta_D}\right)^3\int_o^{\frac{\theta_D}{T}}\frac{y^3}{(e^y-1)}dy\right]. \tag{2-8}$$

Notice that S_M is a function of T only. When $T << \Theta_D$, C_L is proportional to $(T/\Theta_D)^3$, and $_{SL}$ is proportional to $(T/\Theta_D)^3$ as well. Hence, the lattice entropy can be neglected at temperatures much lower than the Debye temperature.

Finally, from Fermi-Dirac statistics theory [51], we know that the conduction electron heat capacity can be expressed as follows.

$$C_E = \gamma T \quad if \quad T << T_F\ , \tag{2-9}$$

where γ is the electronic constant and T_F is the Fermi temperature.

The Fermi temperature of Gd is about 4000 K. The value of γ is about $2.5\text{x}10^{-3}$ cal/mole K. Here the average value of Lanthanum ($2.38\text{x}10^{-3}$) and the value of Lutetium ($2.7\text{x}10^{-3}$) for Gd is taken [52]. Consequently, the conduction electron entropy can be expressed as follows.

$$S_E = \int_o^T \frac{\gamma T}{T}dt = \gamma T \tag{2-10}$$

The total entropy, S_T, is then given by the sum of S_M, S_L, and S_E[1], i.e.,

$$S_T = S_M + S_L + S_E \tag{2-11}$$

The calculated Gd total entropy is plotted on Fig. 2.2 for H = 0, 1, 3, 5, and 7.

3. MAGNETOCALORIC CYCLE ANALYSIS

R. W. Murphy

Based on classical molecular field principles, theoretical models have been developed to provide estimates of magnetization, specific heat, and entropy (shown in Section 2.8 for gadolinium) for a magnetocaloric material within relevant temperature and magnetic field ranges. Comparison of model predictions with gadolinium zero-field specific heat data taken from the literature showed approximate agreement. Review of the resulting entropy tables in the literature indicated a calculational error. Correction of this error provided tables which gave near–Curie-point entropy changes that agreed substantially with those provided by the current theoretical model. For applied magnetic fields of 1–7 T, model predictions of isentropic temperature rise for gadolinium were found to match available data fairly well.

With the theoretical model "validated" within these limited ranges, it was translated into a thermodynamic cycle methodology to allow comparison of four candidate magnetic heat pump approaches for situations with established temperature and magnetic field limits. Each employed isothermal processes at the low-temperature (heat absorption) and high-temperature (heat rejection) extremes. The candidate approaches differed by using constant entropy, constant magnetization, "ideal regenerative," or constant field processes to connect the isothermal portions of the cycles.

The first three candidates give, in principle, "perfect" or Carnot cooling coefficients of performance, but different (increasing in order of listing) cooling capacities. For gadolinium operating between 0 and 7 T in a heat pump cycle with a heat rejection temperature of 320 K, the model predicted a 42% loss in coefficient of performance at 260 K cooling temperature and a 15% loss in capacity at 232 K cooling temperature for the constant field cycle as compared to the ideal regenerative cycle. Such substantial penalties indicate that the potential irreversibilities from this one source may adversely affect the viability of certain proposed MHP concepts if the relevant loss mechanisms are not adequately addressed.

3.1 BASIC CYCLES

Magnetic field work is one in the long list of types of work that can be combined with changes in heat and internal energy to create thermodynamic cycles of practical use, as in heat pumps and heat engines. In place of the pressure and volume variables traditionally employed to represent boundary work, applied magnetic field and magnetization are the variables of choice. To emphasize

heat interactions we will compare cycles based on the temperature-entropy plots for the working material. We start with a brief review of certain cycles in which boundary work is the only form of work considered.

3.1.1 Boundary work cycles

When work is limited to that on the system boundary, the traditional form of the energy equation for the working material is

$$du = T\,ds - p\,dv\,, \tag{3-1}$$

or

$$ds = \frac{du}{T} + \frac{p\,dv}{T}\,, \tag{3-2}$$

where

u is internal energy of the working material,
T its absolute temperature,
s its entropy,
p its pressure,
v its volume.

If we postulate that v is a function only of p/T, it is clear that du/T is a function only of T, and, therefore, that u is a function only of T. One consequence of this result is that the horizontal distance (entropy difference) between any two constant volume lines on T-s coordinates is independent of temperature. If, in particular, we let the function be the equation of state of a semiperfect gas, that is,

$$v = RT/p\,, \tag{3-3}$$

where R is the gas constant, we find in addition that the horizontal distance between any two constant <u>pressure</u> lines on T-s coordinates is also independent of temperature. These relationships are illustrated in Fig. 3.1.

Referring to a graphical representation of these relationships on T-s coordinates, let's look at some traditional refrigeration cycles within specified temperature and pressure boundaries. For each cycle, the heat rejection is given by

$$Q_h = T_h \, \Delta \, s_h , \tag{3-4}$$

the cooling capacity by

$$Q_c = T_l \, \Delta \, s_l , \tag{3-5}$$

the work input by

$$W = Q_h - Q_c , \tag{3-6}$$

and the cooling coefficient of performance by

$$COP_c = Q_c / W , \tag{3-7}$$

where

T_h is the high-temperature limit,

$\Delta \, s_h$ the cycle entropy change at the high-temperature limit,

T_l the low-temperature limit,

$\Delta \, s_l$ the cycle entropy change at the low-temperature limit.

For all the cycles, when the cooling temperature equals the heat rejection temperature, there is no temperature lift, the various types of legs which connect the isothermal legs vanish, and the "cycles" degenerate to a horizontal line (on T-s coordinates), which gives maximum "cooling" capacity with no work input. In this situation, of course, the cooling coefficient of performance is infinite and the heat rejected equals the cooling capacity.

The Carnot cycle, comprised of two isothermal and two isentropic legs as shown in Fig. 3.1, gives maximum efficiency or coefficient of performance, but may be severely limited in capacity when the required temperature lifts are substantial. One way to increase capacity is to employ regeneration (storing and recovering heat) on the nonisothermal legs of the cycle. Perfect regeneration (and the resulting retention of Carnot coefficient of performance) requires reversible storage and recovery of heat (no net entropy generation) which, in turn, implies a fixed horizontal distance between the regeneration process lines on T-s coordinates. Earlier we identified two types of processes that meet this requirement—one (constant volume) as a result of the volume's being solely a function of the ratio of pressure and temperature, and one (constant pressure) as a result of a particular form of that function. Of course, in general, there are other such processes, but they are not so concisely characterized.

The regenerative cycle employing the constant volume processes is traditionally called a Stirling cycle, and that employing the constant pressure processes an Ericsson cycle. From the figure,

it is obvious that, within fixed temperature and pressure constraints, the Stirling cycle can substantially increase the cycle cooling capacity while maintaining a coefficient of performance equal to that of Carnot. Of course, this may require the regenerator to store and furnish significant amounts of heat during the cycle. The figure shows that within the same limits even greater capacity is achievable (and even greater energy storage required) with the Ericsson cycle.

3.1.2 Magnetic work cycles

In the case of magnetic work cycles, we have

$$du = T\,ds + H\,dM,$$

or

$$ds = \frac{du}{T} - \frac{H\,dM}{T},$$

where H is the applied magnetic field and M the magnetization of the material. If we follow the previous line of reasoning and postulate that M is a function only of H/T, it is clear that, once again, du/T is a function only of T, and, therefore, that u is a function only of T. As before, one consequence is that the horizontal distance (entropy difference) between any two constant magnetization lines on T-s coordinates is independent of temperature. If, in particular, we let the function be the equation of state of a semiperfect magnetic substance, that is, one which obeys the Curie Law,

$$M = CH/T,$$

where C is the Curie constant, then we find, in addition, that the horizontal distance between any two constant <u>applied field</u> lines on T-s coordinates is <u>not</u> independent of temperature. These relationships are illustrated in Fig. 3.2.

Thus, the magnetic equivalent of the Stirling cycle in the boundary work example is clearly a cycle composed of two isothermal legs and two isomagnetization legs as shown in Fig. 3.2. As before, such a cycle can, in principle, provide Carnot coefficients of performance with capacities greater than Carnot. Also as before, there are other nonisothermal legs [for example, the low-isofield leg combined with a varying higher-field leg such that the horizontal distance (entropy difference) remains constant through the temperature range] that offer perfect regeneration, but isofield line pairs are not in that group.

If we use a Curie Law material to create a regenerative cycle comprised of two isothermal and two isofield legs, we find that the amount of heat removed from the regenerator exceeds that stored in it—implying that, in the absence of some additional heat source, such a cycle does not represent steady-state system operation. To balance the heat stored in and recovered from the regenerator, the high-field leg must be terminated before the minimum temperature is reached and replaced with a segment of adiabatic demagnetization, as indicated in Fig. 3.2. When compared to the constant magnetization cycle described above, this cycle shows (1) the same amount of heat rejection at the maximum temperature, (2) the same amount of heat stored in and recovered from the regenerator, (3) a smaller amount of heat absorbed from the refrigeration load, and (4) a greater amount of work input to the system. Since the last two results require a reduction in the cooling coefficient of performance, the net effect of going from the ideal regenerative cycle to this cycle is a reduction in both refrigeration figures of merit—capacity and coefficient of performance. In turn, for the present example, these reductions are caused solely by irreversibilities associated with imperfect regeneration.

At this point we must discuss two real-world factors that affect how we extend the examination of magnetic refrigeration cycles. First, even the best currently available magnetic materials operating within the maximum realistic field ranges do not show isentropic temperature rises sufficient to accommodate typical temperature lifts in the room-temperature range. That is, at present even the materials with the greatest magnetocaloric effect will require regenerative cycles for room-temperature applications. Second, the best available materials are those that show ferromagnetic characteristics and have Curie points in the operating-temperature range; that is, they do not obey the Curie Law in the range of interest.

Accordingly, the approach is to (1) implement a model that, while still simple, simulates the important features of realistic material, (2) test the model against available data, and, if the test shows reasonable agreement, (3) use the model to investigate certain cycle loss mechanisms.

3.2 MAGNETOCALORIC MATERIAL MODELING

Consistent with the modeling methodology outlined by Brown [1], the total entropy of the magnetocaloric material was assumed to have three independent additive components: lattice, conduction electron, and magnetic charge (or spin). The first two components were modeled as functions of temperature only (Debye dependence in the first case, proportional dependence in the second). The last component was modeled as a function of temperature and magnetic field according

to methods described by Carlin [2]. Corresponding specific heat components were derived directly from the entropy formulas.

3.2.1 Comparison with existing data

Initially the resulting model was applied to gadolinium with no magnetic field for comparison with the total specific heat data of Griffel et al. [3]. As indicated in Fig. 3.3, the data matched model predictions very well at low temperatures, but fell below the model values at intermediate temperatures. As the Curie region was approached, the data had a substantially sharper peak followed by a considerably more gradual tail than predicted by the model.

Further review of the Griffel paper showed that the entropy table developed from the specific heat data contained an integration error. With this error corrected, reasonable agreement was found between model and experimental values as demonstrated in Fig. 3.4. Comparison of predicted isentropic temperature rises (Fig. 3.5) and isothermal entropy changes (Fig. 3.6) with data-based correlations reported by Benford and Brown [4] showed fair agreement in the temperature range of 194 to 376 K and magnetic field range of 0 to 7 T.

3.3 CYCLE MODELING

Since the model of gadolinium properties was partially validated by the comparisons with experimental data, it was judged adequate to apply to refrigeration cycles of interest to provide simple but realistic bases for judging performance. One such exercise involved fixing the heat rejection temperature (320 K for the example presented here) and magnetic field limits (0–7 T here) while examining the corresponding energy flows and performance parameters for refrigeration, with the cooling temperature varied for (1) a Carnot cycle, (2) a constant magnetization cycle, (3) an ideal regenerative cycle, and (4) a pseudo-constant field cycle.

3.3.1 Carnot cycle

In the case of the Carnot cycle, as the cooling temperature drops below the heat rejection temperature, the available isothermal entropy change (difference between the entropy of the low-temperature, low-field corner and that of the high-temperature, high-field corner of the cycle) decreases rapidly, implying a corresponding rapid decrease in heat rejection, an even more rapid

decrease in cooling capacity, and an increase in work input as shown in Fig. 3.7. At some lower cooling temperature, work input reaches a maximum, while both cooling capacity and heat rejection continue to decrease. At some still lower cooling temperature, the entropy of the low-temperature, low-field corner of the cycle decreases to that of the high-temperature, high-field corner and the "cycle" degenerates to a vertical line that has no cooling capacity, no heat rejection, and no work input. Throughout the cooling-temperature operating range, the Carnot cycle maintains the maximum cooling coefficient of performance, but, as suggested earlier and indicated in Fig. 3.7, for this example the applicable temperature lift is severely limited (zero cooling capacity is reached at approximately 308 K, representing only a 12-K lift to the heat rejection temperature of 320 K).

3.3.2 Constant magnetization cycle

As a consequence of the model employed, two of the additive entropy components are functions of temperature only, while the third is a function of magnetization only. This, in turn, implies that, as for the Curie Law material above, a constant magnetization cycle is capable of "perfect" regeneration and consequent increased cooling capacity while maintaining Carnot coefficient of performance.

From the corresponding numerical example in which the fixed heat rejection temperature has been made higher than the material Curie temperature, as the cooling temperature drops from the heat rejection temperature toward the Curie temperature, the available isothermal entropy change does not vary because we have made the low-field limit zero. This is a direct consequence of the fact that the zero magnetization line coincides with the zero field line above the Curie point. As a result, the heat rejection remains fixed, the cooling capacity falls in a linear fashion, and the work rises linearly as Fig. 3.8 shows. As the cooling temperature drops below the Curie point, the available isothermal entropy change starts to decrease (limited by the now nonzero magnetization of the low-temperature, low-field "corner" of the cycle). In this range, the heat rejection begins to decrease, the cooling capacity decreases more rapidly, and the work input decreases from its maximum until the cooling temperature reaches a value for which the magnetization of the low-temperature, low-field corner equals that of the high-temperature, high-field corner. At this point the "cycle" has collapsed to a single constant magnetization curve that has no cooling capacity, no heat rejection, and no work input.

Thus, in comparison with the Carnot cycle, available cooling capacity and temperature lift have been increased without compromising the cooling coefficient of performance. As before,

however, some reversible provision must be made for the storage and removal of energy during the execution of the constant magnetization legs of the cycle. Unfortunately, although capabilities have been increased substantially over those of Carnot, the numerical example shows that the maximum available temperature lift (that is, the lift at zero cooling capacity) is still only about 42 K.

3.3.3 Ideal regenerative cycle

To take full advantage of the operating region bounded by the established temperature and field limits, it is clear that a different cycle, denoted "ideal regenerative" here, is required. For convenience in illustration, we have let the nonisothermal legs of the ideal regenerative cycle be comprised of a constant low-field (actually zero here) storage path and a varying high-field recovery path that maintains a fixed horizontal separation on the T-s coordinates. For this cycle, we have

$$\Delta s_l = \Delta s_h$$

As the cooling temperature drops from the heat rejection temperature toward the Curie temperature, because we have let the low-field limit be zero, the ideal regenerative cycle coincides with the constant magnetization cycle, and, of course, the respective energy flows and performances are identical. However, Fig. 3.9 indicates that, in contrast to the constant magnetization cycle, both the cooling capacity and the work input remain linear functions of the cooling temperature until the cooling temperature falls far enough below the Curie point such that the corresponding isothermal entropy change between the high- and low-field limits equals that of the heat rejection temperature. As cooling temperature decreases further, the entropy change is set by the (decreasing) low-temperature value, the heat rejection begins to decrease, the cooling capacity falls faster, and the work input increases more slowly. At some lower temperature the work input reaches a maximum, and, from this point on, all three energy quantities decrease toward zero as the cooling temperature approaches absolute zero.

Thus, in principle, the ideal regenerative cycle can extend the minimum cooling temperature toward zero, and, for our example, can give cooling capacities equal to those of the constant magnetization cycle for cooling temperatures above the Curie point and greater than those of the constant magnetization cycle for cooling temperatures below the Curie point. As before, these potential improvements have come while the cooling coefficient of performance was maintained at the "perfect" or Carnot value. Once again, however, some reversible provision must be made for the storage and removal of energy during the execution of the nonisothermal legs of the cycle.

3.3.4 Constant-field cycle

In the case of the constant-field cycle, as the cooling temperature drops from the heat rejection temperature toward the Curie point, the heat rejection again remains fixed while the cooling capacity falls, the work input rises, and the cooling coefficient of performance decreases as shown in Fig. 3.10. However, for this cycle, as was demonstrated earlier for a Curie Law magnetic material, the changes are more rapid than those of the ideal regenerative cycle because of irreversibilities introduced in the regeneration processes. In particular, because an energy balance on the regenerator cannot be maintained by following the high-field leg all the way from the heat rejection temperature to the cooling temperature, the leg must be terminated and replaced with a segment of adiabatic demagnetization before the cooling temperature is reached. As shown previously, when compared with the ideal regenerative cycle described above, this constraint results in (1) a smaller entropy change during the isothermal leg at the cooling temperature, (2) a reduced cooling capacity, (3) a greater amount of work input to the cycle, and (4) a smaller cooling coefficient of performance.

As the cooling temperature passes through the Curie point, the shapes, but not the trends, of the curves change. From the previous discussion it should be recalled that, according to the model employed here, the zero-field specific heat undergoes a step increase as the Curie point is reached from above. In particular, at this temperature the value changes from one smaller than the high-field value to one greater than the high-field value. In other words, below the Curie point the material at zero field can absorb more heat over a given temperature interval than can the material at high-field. Of course, the reverse is true above the Curie point. A consequence of this is that, below the Curie point, as the cooling temperature decreases, the portion of high constant-field line that must be replaced by the adiabatic demagnetization leg is progressively reduced until some lower temperature is reached where no adiabatic demagnetization portion is required at all. At this point and for all lower temperatures, the cooling capacity of the constant-field cycle equals that of the ideal regenerative cycle. However, for lower temperatures the regenerator energy balance requirement leads to termination of the low-field (zero) line below the heat rejection temperature and insertion of an adiabatic magnetization leg to complete the cycle. A direct result of the insertion of an adiabatic magnetization leg is a decrease in heat rejection.

In summary, for the example here the constant-field cycle also extends the minimum cooling temperature toward zero, but, when compared with the ideal regenerative example, it does so with reduced refrigeration capacity within some of that range and with reduced cooling coefficient of performance within the entire range. These trends are illustrated in Fig. 3.11, which shows, for

example, a 42% loss in coefficient of performance at 260 K cooling temperature and a 15% loss in capacity at 232 K cooling temperature for the constant-field cycle as compared with the ideal regenerative cycle. The comparative cycles for these two conditions are presented on temperature-entropy coordinates in Figs. 3.12 and 3.13. In any real device many other loss mechanisms can affect cooling performance, but such substantial penalties indicate that the potential irreversibilities from this one source may adversely affect the viability of certain proposed MHP concepts if the relevant loss mechanisms are not adequately addressed.

4. CYCLE ENERGY LOSSES

V. C. Mei and G. L. Chen

In addition to the intrinsic energy inefficiency related to cycle selections, an MHP will experience many other losses as well. In this section, the heat transfer mechanism of a reciprocating MHP system is derived. Several losses, such as those caused by eddy current, magnetic hysteresis, and demagnetization, are calculated or estimated. Finally, the induced magnetic force on a Gd core is calculated, which indicates that moving a core in and out of a strong magnetic field could be difficult because of the huge magnetic force on the core material.

4.1 MODEL OF HEAT TRANSFER BETWEEN MAGNETIC MATERIALS AND REGENERATOR FLUID

The basic concept of an MHP is that the magnetic material can be heated up or cooled down by the application or removal of an external magnetic field, and can dissipate heat to or absorb heat from the regenerator. Hence, understanding the heat transfer between the magnetic material and the regenerator fluid is vital in real system design. In this section, we derive a heat transfer model for the MHP system. The core material is considered as a porous bed in this model. Gd is considered to be the magnetic core material. The regenerator tube is filled with fluid and reciprocated up (heat reservoir) and down (cold reservoir). Alternately, the core can be stationary and the regenerative fluid can be pushed up and down reciprocatively. The following energy balance equations are used to govern the system:

Fluid—

$$\alpha \rho_f C_f \frac{\partial T}{\partial t} = -V_f \rho_f C_f \frac{\partial T}{\partial x} + hA(\theta - T) \tag{4-1}$$

Gd—

$$(1-\alpha)\rho_s C_s \frac{\partial \theta}{\partial t} = hA(T-\theta) + (1-\alpha)\lambda_s \frac{\partial^2 \theta}{\partial x^2} \tag{4-2}$$

$$+\frac{1}{t}\int_o^t \frac{Q_1}{\Delta t_1}\delta(t-t_1)dt + \frac{1}{t}\int_o^t \frac{Q_2}{\Delta t_2}\delta(t-t_2)dt$$

where

α is the porosity,

ρ_f and ρ_s are the densities of fluid and Gd, respectively,

t is time,

x is the horizontal coordinate of the porous bed,

C_f and C_s are the fluid and Gd heat capacities, respectively,

V_f is the fluid flow rate,

T is the fluid temperature,

Θ is the Gd temperature,

h is the conductance between the fluid and Gd,

A is the contact area per unit volume of Gd.

λ_s is the effective axial thermal conductivity of Gd.

The last two terms in Eq. 4-2 are the source and sink terms, which represent the magnetization and demagnetization processes during which the Gd core temperature changes, where Q_1 and Q_2 are the quantity of heat released or absorbed when the core is magnetized or demagnetized. Δt_1 and Δt_2 are the times needed to complete the magnetization and demagnetization processes, respectively. Equations 4-1 and 4-2 were solved numerically. The parameters are listed in Table 4.1.

Table 4.1. Equation parameters

Value	Parameter		Units
α	0.4		—
h	0.99	(237.65)	cal/sec-cm^2-°C (Btu/h-ft^2-°F)
A	0.17	(5.2)	cm^{-1}(ft^{-1})
ρ_f	0.99	(62.4)	g/cm^3 (lb/ft^3)
C_f	0.31	(1.00)	cal/g-°C (Btu/lb-°F)
V_f	3.39	(400.00)	cm/sec (ft/h)
ρ_s	7.86	(491.00)	g/cm^3 (lb/fT^3)
C_s	0.017	(0.055)	cal/g-°C (Btu/lb-°F)
λ_s	0.66	(5.20)	cal/sec-cm-°C (Btu/h-ft-°F)

The numerical results of temperature profiles of fluid and Gd are shown for four different process stages in Figs. 4.1, 4.2, 4.3, and 4.4. The cycle starts with magnetizing Gd with no fluid movement. The Gd increases in temperature at this stage as shown in Fig. 4.1. Then the regenerator fluid flows through the Gd and absorbs heat from it (Fig. 4.2). Demagnetization then decreases the Gd temperature (Fig. 4.3). After demagnetization, the fluid flows back from the left and warms up the Gd.

4.2 HEAT LOSSES

Heat loss is one of the important factors related to machine design and operation. Heat losses must be calculated or estimated before a system can be realistically designed. Kirol et al. [1] analyzed some loss mechanisms in detail based on the second law of thermodynamics. Appendix C provides an example of the loss calculation. Here, some of the losses not mentioned by Kirol's report are studied, namely eddy current loss, magnetic hysteresis loss, and demagnetization field loss. Some losses, such as loss caused by temperature difference between magnetic core material and fluid, conduction heat transfer within core material, etc., are actually included in Equations (4-1) and (4-2). Some other losses, such as fluid mixture caused by turbulence and heat leaks through walls, are not included in this study for the time being because they involve heat pump design and operating conditions.

4.2.1 Eddy current loss

Eddy current will be induced in magnetic metals when the magnetic field is varied. The eddy current loss per cm^3 in cylindrical matter with sinusoidally varying external magnetic fields can be expressed as follows.

$$P_e = \frac{\pi^2 d^2 B^2 f^2}{16 \rho C^2} , \tag{4-3}$$

where

d is diameter of the cylinder,

ρ is resistivity (140.5×10^{-6} ohm-m at 20°C),

c is the speed of light (3×10^{10} cm/s),

f is frequency of cycling,

B is magnetic induction (7×10^4).

Since the Gd core for this study can be approximately represented by a 4-in. long, 2-in. diameter cylinder, the total power loss per cycle (P_e x volume) will be 0.76 J/cycle if f=4 and B=7 T.

Equation (4-3) suggests that the eddy current loss is proportional to the square of diameter, frequency, and magnetic field. The loss is small for low-frequency operation. When the frequency increases, the loss increases rapidly. Reducing the core material diameter would reduce the loss, as would laminating the core.

4.2.2 Magnetic hysteresis loss

The amount of energy loss associated with magnetic hysteresis is readily determined from the hysteresis loop area. But the shape of the hysteresis loop is affected by many factors, such as gross composition, heat treatment, impurities, temperature, fabrication, stress, etc. Since we do not have Gd hysteresis loop data, the loop is assumed to be that of pure iron as an approximation. According to the law of Steinmetz for high fields from 0.5 to 15 Tesla [2], the hysteresis loss of pure iron (annealed at 900° C) is as follows.

$$P_h = 1.2 \times 10^{-3} B^{1.6} \tag{4-4}$$

Hence, the total hysteresis loss (P_h x volume) of Gd core for this study in a 7-T field will be 1.4 J per cycle, twice as high as eddy current loss. However, this loss can be significantly reduced (by several orders of magnitude) by annealing, purifying, and fine fabricating when the Gd core is prepared.

4.2.3 Demagnetization field

A magnetized finite-size magnetic material can produce an inner magnetic field in the opposite direction from the external field. This is called the demagnetizing field. Hence, the true field inside a magnetic material could be reduced by the demagnetization factor (D). (This factor depends primarily on the shape of the magnetic material [2].) The true field can be written as follows.

$$H_t = H_a - DM, \tag{4-5}$$

where

H_t is the true magnetic field,

H_a is the applied magnetic field,

M is magnetization.

For a cylinder with a dimension ratio (length/diameter) of 2, D is 0.14, which implies that the demagnetization field is about 14% of saturated magnetization. However, D varies from place to place in the material, decreasing from the middle section of the core toward the ends. To reduce the demagnetization field, the Gd core should be designed for a large dimension ratio because the value

of D decreases as the dimension ratio increases. Table 4.2 lists the experimentally determined demagnetizing factors for cylindrical specimens with different dimension ratios.

Table 4.2. Demagnetizing factors for cylindrical specimens

Dimensional ratio	Demagnetizing factor
0	1.0
1	0.27
2	0.14
5	0.040
10	0.0172
20	0.00617
50	0.00129
100	0.00036
1000	0.0000036

4.2.4 Magnetic force induced by external field on the gadolinium core

From Ampère's law, we know that a magnetic force is created on a magnetic material when it is exposed to an external magnetic field. This force could be very strong in a high magnetic field. To design a heat pump system with a core moving in and out of a magnetic field, one must first calculate this force.

Consider a magnetic material that has magnetization M inside a volume V bounded by a surface S:
in a uniform B_e field, the adhesive force on this body can be calculated as follows [3].

$$\bar{F} = -\int_V (V.\vec{M})\vec{B}_e \, dV + \int_s (\vec{M}\vec{N})\vec{B}_e \, dS \ , \tag{4-6}$$

where $\vec{N}$ is the unit normal vector. If this body has a right circular cylinder with length L and diameter d, and the long axis is parallel to the field B_e, the force is

$$F = \pi M B_e d^2/2 \ . \tag{4-7}$$

It is interesting that the force is independent of core length.

Near room temperature, Gd has an M of 0.86 J/T-cm^2. Hence, for the Gd core considered in this study (2-in. diameter and 4-in. length), F = 244 J/cm (24,400 N or 5485 lbs) in a 7-T field. Under this huge magnetic force, a fixed core seems more appropriate than a core moving in and out of the magnetic field.

5. PULSED DC MAGNET ANALYSIS

J. W. Lue and M. S. Lubell

In order to operate an ideal regeneration MHP cycle using a single-component working medium, pulsed DC magnets will be needed. Three aspects of the project regarding the superconducting magnets have been pursued during this report period. A superconducting pulse magnet has been designed for the next step of the heat pump experiment. The ac losses of such a magnet and of the magnet used in the previous test have been analyzed. Finally, a review has been undertaken of the energy transfer schemes for a tandem MHP system that uses two superconducting magnets.

5.1 PULSE MAGNET DESIGN

The preliminary heat pump experiment reported earlier showed that pulsing a magnetic field on a stationary magnetic sample is a good way to achieve the heat pump function. However, the magnet used in that test was reconfigured from a magnet designed for dc operation. The pulse rate is limited and the loss is high. Based on the available Gd sample, a more compact, fast-pulsed, high-field magnet has been designed.

A magnet with a bore of 9.0 cm (3.5 in.), an OD of 21 cm (8.3 in.), and a length of 30.5 cm (12 in.) is designed to produce an 8-T dc field at a current density of 12 kA/cm^2. Such a magnet can then be pulsed stably to 7 T in 0.5 s and down in 0.5 s. A dewar with a reentrant warm bore can provide a 6.3-cm (2.5 in.) bore clear through the working space for the sample. The field uniformity is within 95% in the 10-cm (4 in.) long working space. It is also estimated that such a magnet system including magnet, dewar, leads, and holding structure can be built for $60,000. This price is further confirmed by a private manufacturer. The firm actually said that by using a higher current density they can build the magnet system for more than $10,000 below our estimate.

The energy storage of this magnet at a 7-T field is about 200 kJ. To ramp it up in 0.5 s requires a power supply rating of at least 800 kW with a current output on the order of 1 kA. Such a power supply could cost twice as much as the magnet system estimated above. ORNL has a motor-generator which can supply 350 V and 8670 A to the magnet laboratory. Thus, a magnet built with a 2.5-kA or bigger conductor can be powered readily by the existing facility.

5.2 AC LOSS ANALYSIS

When a superconducting magnet is pulsed or operated in an ac mode, several mechanisms cause energy loss in the magnet. These include hysteresis loss in the superconductor, coupling loss in the stabilizer of the superconducting strands, eddy current loss in the cable, and eddy current loss in the conductor conduit and the coil case. The hysteresis loss comes from work against the pinning force as the magnetic field sweeps through the superconductor. It is proportional to the superconductor critical current density, the filament size, and the magnitude of the field sweep. It does not depend on the sweep rate. The coupling loss comes from induced currents flowing across the stabilizer between superconducting filaments. It is proportional to the square of the field sweeping rate and the filament twist pitch, and is inversely proportional to the resistivity of the stabilizer. The eddy current loss is proportional to the square of the field sweeping rate and the dimension of the metal, and is inversely proportional to the resistivity of the metal.

The cable-in-conduit magnet used in the preliminary MHP test was charged up to 7 T and down in a 30 s period to measure loss rate. Numerical calculations resulted in a hysteresis loss of 160 J, a coupling loss of 20 J, an eddy current loss of 1–52 J in the cable (depending on how well the strands are electrically coupled to each other), and an eddy current loss of 8 J per cycle in the conduit and the coil case. Thus, there is a total ac loss of 189–240 J. For a continuous cycle at this period, this loss would boil off 9–11 L/h of helium. The loss from the large 5-kA leads used for that magnet and other background loss was about 16 L/h. Thus, a loss rate of 25–27 L/h was calculated. This compared very well with the measured 23 L/h. Similar calculations resulted in 23–24 L/h for the 5-T, 30-s period run as compared with the measured 24 L/h, and 27–30 L/h for the 5-T, 20-s period run as compared with the measured 17 L/h. The last measured value is quite far off. It is not clear why, except that lead cooling might have changed considerably during that run.

It is significant that the hysteresis loss was the dominant ac loss for the ramp period used before. If that magnet were to ramp up to 7 T and down in a 1.0-s period, the situation would be changed completely. The hysteresis loss would remain at 160 J, but the coupling and eddy current loss would all go up by a factor of 30. Thus, a total of 1030–2560 J per cycle of ac loss could be expected. The big uncertainty comes from the eddy current loss in the cable, because the strands are not insulated and the degree of coupling among them are unknown. The two values quoted are for the extremes of insulated and completely coupled. This ac loss will boil off 1400–3500 L/h of liquid helium in a continuous cycle. Therefore, it is impractical to run a heat pump experiment with that

magnet at this cycle rate continuously. Notice also that at this ramp rate the lead and background loss become negligible compared to the ac losses.

Applying the above ac loss analysis to the presently designed pulse magnet, one can find a few ways to reduce the loss. The hysteresis loss can be reduced by using smaller superconducting filament. A reduction factor of two is quite practical. Using a tighter twist pitch and a resistive barrier in the stabilizer can reduce the coupling by a factor of five or more. Insulation or resistive barriers between strands can limit eddy current loss in the cable to individual strands. Considering these factors, a total loss of about 300 J or less per 1.0-s cycle should be achievable with this pulse magnet. This amounts to losing about 0.15% of the stored magnetic energy to the helium environment.

5.3 TANDEM SYSTEM CONSIDERATION

Pulsing the magnetic field to harness the magnetic cooling effect alleviates the very difficult mechanical problem of moving the magnetic material in and out of the field. However, large magnetic energy is being charged to and discharged from the magnet. For the system to be energy efficient, the discharged energy must be saved for reuse. One possible scheme is to devise a tandem system in which two heat pump units are run in sequence. The energy being discharged from one magnet is transferred to the magnet of the other unit and then transferred back to the first magnet in the beginning of the next cycle. Thus, the magnetic energy is conserved and transferred back and forth between the magnets. Only some energy losses such as the ac loss discussed previously need to be made up. Furthermore, a high-power power supply is not needed in this scheme.

Methods for transferring energy between superconducting magnets have been studied for superconducting magnetic energy storage systems and for powering accelerator magnets and the poloidal field coils of a Tokamak fusion reactor [1]. Transfer by electronically switched small capacitors seems to be most promising and can be readily adapted to the present application. Three major variations of the electronic switching method have been proposed: the flying capacitor circuit by the Karlsruhe group, the dual inductor-converter bridge by the Wisconsin group, and the chopper circuit by the Electrotechnical laboratory in Japan.

The design principles of these solid state transfer circuits are basically the same. The Karlsruhe circuit consists of one capacitor and two thyristor units. The m-phase Wisconsin circuit consists of m capacitors and 4m thyristor units. The more complex third scheme has the advantage of increasing the number of transfer steps at a lower frequency of the transfer circuit, thus reducing

the problems of current rise rate and the acceptable transfer circuit inductance. A single-phase dual converter scheme has also been investigated to simplify and enhance the reliability of the inductor-converter bridge circuit [2]. The Electrotechnical circuit consists of one capacitor and two chopper units. It was shown to be able to transfer energy at a lower voltage and higher speed than the flying capacitor scheme.

A group at KEK (a high-energy physics laboratory in Japan) has used the dual inductor-converter bridge circuit to successfully transfer magnetic energy between two 100-kJ superconducting coils [3]. They also found that the main losses in the energy transfer were caused by the thyristor forward voltage drops, the protection resistors, and the circuit cables. A transfer efficiency of about 80% was obtained at a transfer time of 2 s. Since the thyristor loss is linearly proportional to current, and the energy increases as current squared, the efficiency should improve at higher energy ratings. The Electrotechnical group used a chopper circuit to transfer energy reversibly between a 4-MJ storage magnet and a 3-MJ load magnet [4]. Transfer time as short as 1.5 s was achieved in transferring 2.5 MJ of energy from one magnet to the other. At this rate, they measured an ac loss in the load magnet of less than 0.2% of the stored energy (about the same magnitude as that estimated for the presently designed pulse magnet) for the field sweep of 0–5.9 T in 3 s. A transfer efficiency of about 93% was reported in that study.

6. CONCLUSIONS AND RECOMMENDATIONS

MHPs, in principle, could be simple, efficient, and reliable. MHPs can have wide applications, such as process heating, refrigeration, food processing (at 220 K), chemical manufacturing (160 K), liquid hydrogen (20 K) production, and cryogenic cooling from liquid nitrogen (77 K) to liquid helium temperatures. Potential energy savings could be on the order of 5–9 billion kWh per year in the industrial sector alone, according to a 1987 study [1]. A possible early market for the technology could be in the industrial gas supply area, such as the production of liquid hydrogen.

The technology of MHP is in its embryonic stage. While progress has been made in recent years, many gaps exist in scientific and engineering knowledge, limiting the development of MHPs. This study examined thermodynamic cycles and a number of energy loss mechanisms, but is by no means comprehensive. The large magnetic force experienced by the rotary and reciprocating designs was identified by the system development studies in the past [2, 3]; we took a different approach. Our emphasis was on system analysis and testing to explore the mechanically static concept in which the working medium will be stationary. The heat transfer in the regenerator will be similar among the different system concepts, but the system power-loss mechanisms will be different. Magnets will be operating in a continuous mode in rotary or reciprocating MHPs, but in a pulsed mode in mechanically static MHPs. The power losses for a pulsed magnet have been examined.

The following conclusions and recommendations may be drawn from the study:

1. Much of the previous work on MHPs identified by the literature survey focuses on very low temperature (around 4 K) applications. Studies of MHPs for applications in other temperature ranges are a recent development and references are few. To further the MHP technology, expanded research and development efforts are needed.
2. From the thermodynamic cycle viewpoint, the magnetic Carnot cycle should be employed if the temperature lift in an MHP is small. On the other hand, the ideal magnetic regenerative cycle would be a proper choice for large temperature lifts. Proper selection of thermomagnetic (TM) materials and intended application temperature ranges need to be examined to avoid intrinsic cycle losses before a system design is implemented. To that end, the database of thermophysical properties of T working materials needs to be developed.
3. We examined several types of heat loss caused by thermomagnetic interactions between the magnetic field and working medium that had not been analyzed previously, including eddy current, hysteresis, and demagnetization losses. However, one of the major heat losses in an

MHP will be in the regenerator. Depending on the operating conditions, the heat flux in a regenerator is several times that of the cooling load. Efficient regenerator design is a must for regenerative MHPs. Based on the previous studies, a regenerator heat-transfer model was modified to simulate the energy flow between the porous working medium and the regenerator fluid. To understand the active regenerative heat-transfer phenomena, and, further, to derive optimum regenerator design methodology for various applications and configurations are two of the most critical needs for making MHPs a viable technology. The understanding of loss should be pursued actively.

4. The ac loss for a superconducting pulse magnet intended for the test facility for magnetic regenerative heat transfer is projected to be as low as 0.15% of the stored magnetic energy. Research in pulse magnet design, efficient power transfer between coils, and uses for new high-temperature superconducting materials is an integral part of the MHP technology and should be investigated in a timely manner.

REFERENCES

Section 1

1. F. Giauque, *J. Am. Chem. Soc.* **49** (1870).
2. P. DeBye, *Ann. Physik* **81**, 1154 (1926).
3. F. Giauque and D. P. MacDougall, *Phys. Rev.* **43**, 768 (1933).
4. J. G. Daunt and C. V. Heer, *Phys. Rev.* **76**, 854 (1949).
5. G. V. Brown, *J. Appl. Phys.* **47**(8), 3674 (1976).
6. J. A. Barclay and W. A. Stegert, "Magnetic Refrigerator Development," EPRI Report EL-1757, 1981.
7. J. I. Mills et al., "Magnetic Heat Pump Cycles for Industrial Waste Heat Recovery," *Proc. 19th IECEC*, 1369 (1984).
8. L. D. Kirol et al., "Magnetic Heat Pump Feasibility Assessment," Idaho Natl. Engineering Lab. EGG-2343, 1984.

Section 2

1. J. A. Barclay, "Magnetic Refrigeration: A Review of a Developing Technology," *Advances in Cryogenic Engineering*, Vol. 33, pp. 719-731, ed. R. W. Fast, Plenum Press, 1987.
2. EA-Mueller, Inc., *Cost and Availability of Magnetic Heat Pump Materials*, EA-M Project No. 87-604-98 report, prepared for U.S. Dept. of Energy, Office of Industrial Programs, Jan. 1989.
3. H. B. Callen, *Thermodynamics*, Wiley, N. Y., 1959.
4. J. A. Stratton, *Electromagnetic Theory*, Ch. 11, McGraw Hill, N. Y., 1941.
5. J. A. Barclay, "The Theory of an Active Magnetic Regenerative Refrigerator," *Proc. Second Biennial Conference on Refrigeration for Cryogenic Sensors and Electronic Systems*, Goddard Space Flight Center, Greenbelt, Md., Dec. 7 and 8, 1982.
6. A. V. Larson et al., *Feasibility Analysis of Reciprocating Magnetic Heat Pumps*, Semiannual Status Report for the period 7/3/85 to 1/2/86 to NASA, Georgia Institute of Technology, Atlanta, Ga.
7. G. V. Brown, "The Practical Use of Magnetic Cooling," *Proc. 13th International Congress of Refrigeration*, pp. 587-592, International Institute of Refrigeration, Washington, D.C., 1971.
8. G. V. Brown, "Magnetic Heat Pumping Near Room Temperature," *J. Applied Physics* **47**, No. 8, 3673-3680 (Aug. 1976).
9. H. Oesterreicher and F. T. Parker, "Magnetic Cooling Near Curie Temperature Above 300 K," *J. Applied Phys.* 55(12), 4334-4338 (June 1984).
10. A. H. Morrish, *The Physical Principles of Magnetism*, pp. 70–73, Wiley, 1965.
11. G. V. Brown, "Magnetic Stirling Cycles -- A New Application for Magnetic Materials," *IEEE Trans. on Magnetics* **Mag-13**, No. 5, 1146-1148 (Sept. 1977).
12. F. C. Chen, *Study of Superconducting Magnetic Heat Pumping*, Oak Ridge Natl. Lab., unpublished data, Oct. 30, 1989.
13. L. D. Kirol et al., *Magnetic Heat Pump Feasibility Assessment*, EGG-2343 report prepared for DOE, EG & G Idaho, Inc., Idaho Falls, Idaho.

14. K. Matsumoto et al., "An Ericsson Magnetic Refrigerator for Low Temperature," *Advances in Cryogenic Engineering*, Vol. 33, pp. 743-750, ed. R. W. Fast, Plenum Press, 1987.
15. L. D. Jennings et al., "Heat Capacity of Thulium from 15 to 360 K," *J. Chem. Phys.* **34**, 2082 (1961).
16. R. E. Skicgdopole et al., "Heat Capacity of Erbium from 15 to 300 K," *J. Chem. Phys.*, **23**, 2258 (1955).
17. C. B. Zimm et al., "The Magnetocaloric Effect in Erbium," *Proc. International Cryocooler Conference*, pp. 49-57, Aug. 18-19, 1988, Naval Postgraduate School, Monterey, Calif.
18. B. C. Gerstein et al., "Heat Capacity of Europium from 5 to 300 K," *J. Chem. Phys.* **47**, 5149 (1967).
19. G. Green et al., "The Magnetocaloric Effect of Some Rare Earth Metals," *Advances in Cryogenic Engineering*, Vol. 33, p. 777, 1988.
20. B. C. Gerstein et al., "Heat Capacity of Holmium from 15 to 300 K," *J. Chem. Phys.* **27**, 394 (1957).
21. S. M. Benford, "The Magnetocaloric Effect in Dysprosium," *J. Appl. Phys.* **50**, 1868–1870 (1979).
22. R. M. Jennings et al., "Heat Capacity of Terbium from 15 to 300 K," *J. Chem. Phys.* **27**, 2258 (1957).
23. S. M. Benford and G. V. Brown, "T-S Diagram for Gadolinium Near the Curie Temperature," *J. Appl. Phys.* **52**(3), 2110-2112 (March 1981).
24. Personal communication between V. C. Mei (ORNL) and G. Green, David Taylor R&D Center, Bethesda, Md., April 1989.
25. T. Hashimoto et al., "Recent Progress in Magnetic Refrigeration Studies," *Advances in Cryogenic Engineering*, Vol. 33, pp. 733-741, Plenum, N. Y., 1988.
26. *Handbook on the Physics and Chemistry of Rare Earth*, ed. K. A. Gechneider and L. Eyring, Ch. 7, p. 523, North Holland, 1978.
27. C. B. Zimm and P. M. Ratzmann, *The Magnetocaloric Effect in Neodymium*, David Taylor R & D Center Final Report, May 11, 1989.
28. S. A. Nikitin et al., "MCE in Precious Alloys," *Physics, Metals and Metallurgy* **59**, No. 21 (1985).
29. S. A. Nikitin et al., "MCE in Monocrystal Terbium and its Alloy with Gadolinium," *Physics, Metals and Metallurgy* **66**, No. 1 (1988).
30. S. A. Nikitin and A. M. Tishin, "Determining Specific Heat of Magnetic Refrigerants Based on Precious Metals and Their Alloys by Measuring MCE," letter to *JTF* **14**, No. 8 (April 26, 1988).
31. U.S. Congress, *Strategic Materials: Technologies to Reduce U.S. Import Vulnerability*, Report No. OTA-ITE-248, Office of Technology Assessment, Washington, D.C., May 1985.
32. *Handbook of Thermophysical Properties of Solid Materials*, Vol. 1, *Elements*, ed. A. Goldsmith et al., Pergamon, 1961.
33. H. E. Nigh et al., "Magnetization and Electrical Resistivity of Gadolinium Single Crystals," *Physical Review* **132**, No. 3, 1092-1097 (Nov. 1963).
34. M. Sahashi et al., "Specific Heat and Magnetic Entropy Associated with Magnetic Ordering in Al-Rich RAl_2 Sintered Compounds," *IEEE Trans. on Magnetics* **23**(5), 2853-2855 (Sept. 1987).
35. R. Hashimoto, "New Application of Complex Magnetic Materials to the Magnetic Refrigerant in an Ericsson Magnetic Refrigerator," *J. Appl. Phys.* **62**(9), 3873-3878 (Nov. 1987).
36. R. Hashimoto et al., "A New Method for Producing the Magnetic Refrigerant Suitable for the Ericsson Magnetic Refrigerator," *IEEE Trans. on Magnetics* **23**(5), 2847-2849 (Sept. 1987).
37. C. B. Zimm et al., "Measured Properties of GdNi for Magnetic Refrigeration Applications," *Advances in Cryogenic Engineering*, ed. R. W. Fast, Vol. 33, 791-798, Plenum, N. Y., 1988.
38. G. V. Brown, "Basic Principles and Possible Configurations of Magnetic Heat Pumps," *ASHRAE Trans.* **87** (Pt. 2), (1981).

39. C. R. Cross et al., "Optimal Temperature-Entropy Curves for Magnetic Refrigeration," *Advances in Cryogenic Engineering*, ed. R. W. Fast, Vol. 33, pp. 767–775, Plenum, N. Y., 1988.
40. G. V. Brown and S. S. Papell, "Regeneration Tests of a Room Temperature Magnetic Refrigerator and Heat Pump," unpublished paper, NASA Lewis Research Center, Cleveland, Ohio, 1977.
41. K. Matsumoto et al., "An Ericsson Magnetic Refrigerator for Low Temperature," Advances in Cryogenic Engineering, ed. R. W. Fast, Vol. 33, pp. 743–750, Plenum, N.Y. 1988.
42. J. R. Hull and K. L. Uherka, "Magnetic Heat Pumps for Near-Room-Temperature Applications," *Energy* **14**, No. 4, 177-185 (1989).
43. S. R. Jaeger et al., "Analysis of Magnetic Refrigeration with External Regeneration," *Advances in Cryogenic Engineering*, ed. R. W. Fast, Vol. 33, pp. 751–755, Plenum, N.Y., 1988.
44. G. Green and E. Schroeder, "A Finite Element Model of an Experimental Magnetocaloric Refrigerator," *Proc. of International Cryocooler Conference*, pp. 69-80, Aug. 18-19, 1988, Naval Postgraduate School, Monterey, Calif.
45. F. Brailsford, "Theory of a Ferromagnetic Heat Engine," *Proc. IEE* **111**, No. 9, 1602–1606 (Sept. 1964).
46. L. D. Kirol and Dacus, "Rotary Recuperative Magnetic Heat Pump," *Advances in Cryogenic Engineering*, ed. R. W. Fast, Vol. 33, pp. 757–765, Plenum, N.Y., 1988.
47. B. J. Beaudry, "Preparation and Fabrication of Rare Earth Magnetic Materials," *Advances in Cryogenic Engineering*, ed. R. W. Fast, Vol. 33, pp. 785–790, Plenum, N.Y., 1988.
48. S. H. Castles, "Current Developments in NASA Cryogenic Cooler Technology," *Advances in Cryogenic Engineering*, ed. R. W. Fast, Vol. 33, pp. 799–807, Plenum, N.Y., 1988.
49. M. Griffel, R. E. Skochdopole, and F. H. Spedding, "The Heat Capacity of Gadolinium from 50 to 355 K," *Phys. Rev.* **93**, 657 (1954).
50. A. H. Morris, *Physical Principles of Magnetism*, Wiley, N.Y., 1965.
51. F. Reif, *Fundamentals of Statistical and Thermal Physics*, McGraw Hill, N.Y., 1965.
52. M. W. Zemansky, *Heat and Thermodynamics*, 5th ed., McGraw Hill, N.Y., 1968.

Section 3

1. Same as ref. 8 in Section 2.
2. R. L. Carlin and A. J. Duyneveldt, *Magnetic Properties of Transient Metal Compounds*, Springer-Verlag, N. Y., 1977.
3. Same as ref. 5 in Section 2.
4. Same as ref. 23 in Section 2.

Section 4

1. L. D. Kirol et al., *Magnetic Heat Pump Feasibility Assessment*, Idaho Natl. Engineering Lab. Report No. EGG-2343, 1984.
2. R. M. Bozorth, *Ferromagnetism*, Van Nortrand, Princeton, N. J., 1951.
3. J. D. Jackson, *Classical Electrodynamics*, 2nd ed., Wiley, 1975.

Section 5

1. R. S. Ramshaw and E. P. Dick, "Energy Transfer Masses Between Superconducting Magnets," Advances in Cryogenic Engineering, ed. R. W. Fast, Vol. 21, pp. 149-156, Plenum, Nl Y., 1976.
2. M. Ehsani, R. L. Kustom, and R. W. Boom, *IEEE Transactions On Magnetics* **MAG-21**, No. 2, 1115 (1985).
3. M. Masuda, T. Shintomi, and K. Asaji, "Energy Transfer in the System of Superconductive Magnets," Advances in Cryogenic Engineering, ed. R. W. Fast, Vol. 25, pp. 61-68, Plenum, N. Y., 1980.
4. T. Onishi et al., IEEE Transactions on Magnetics **MAG-21**, No. 2, 1107 (1985).

Section 6

1. Same as ref. 2 in Section 2.
2. Same as ref. 6 in Section 1.
3. Same as ref. 8 in Section 1.

FIGURES

ORNL-DWG 90-11955

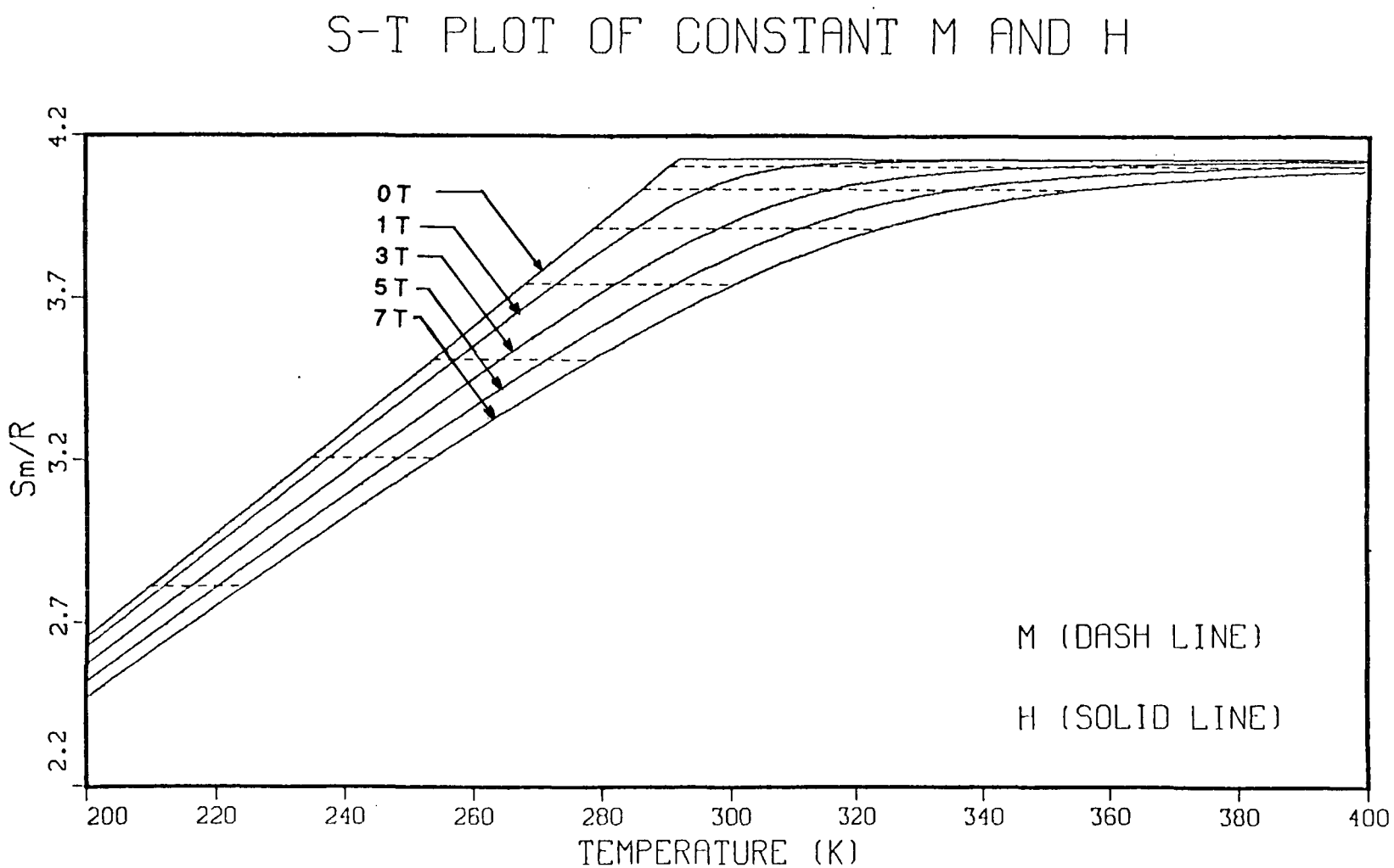

Fig. 2.1. Spin entropy as a function of temperature and magnetic field.

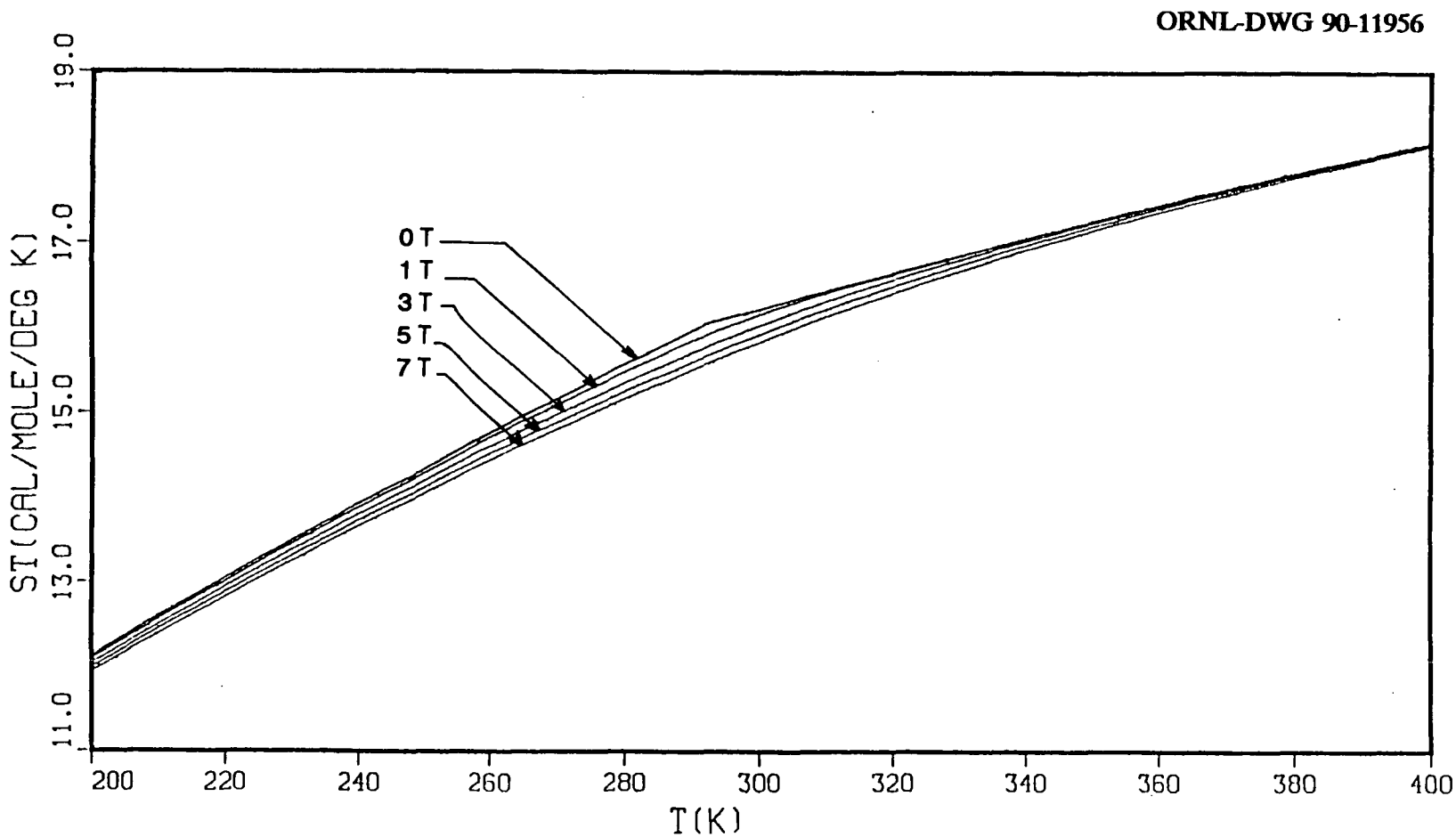

Fig. 2.2. Total entropy as a function of temperature and magnetic field.

ORNL-DWG 90-11717

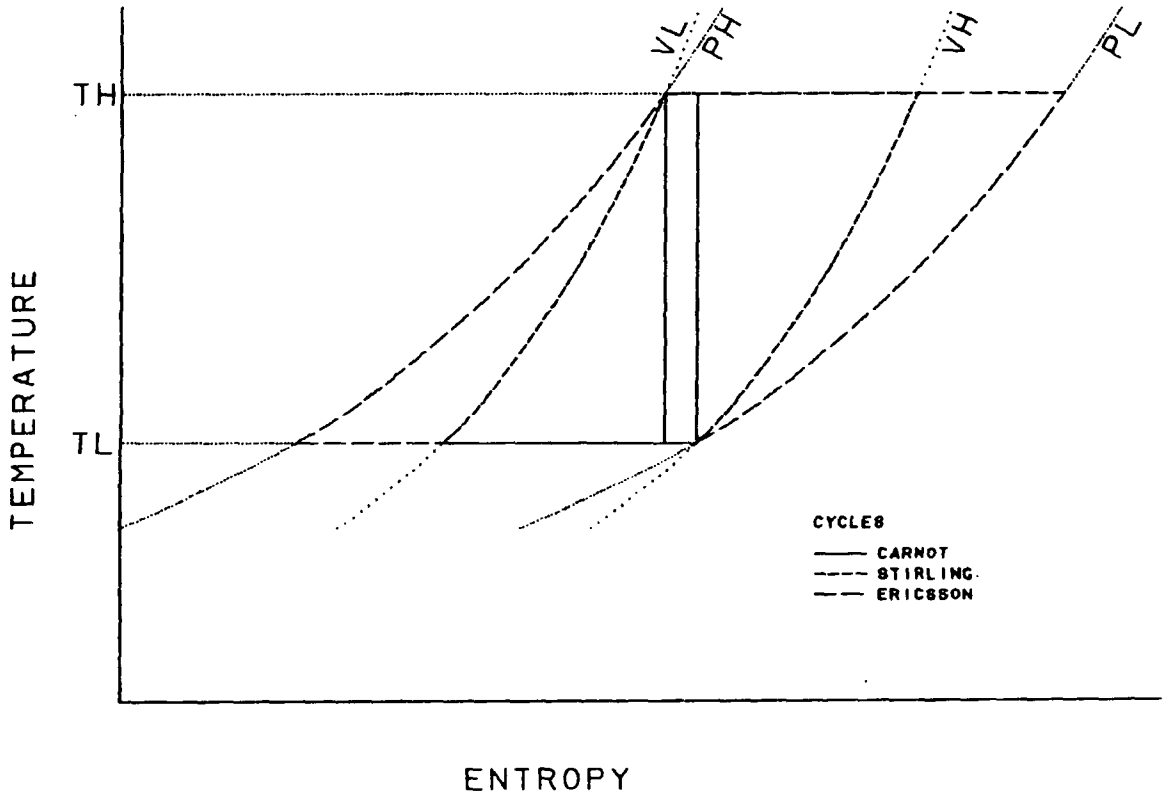

Fig. 3.1. T-s with constant volume and pressure lines; Carnot, Stirling, and Ericsson cycles.

ORNL-DWG 90-11718

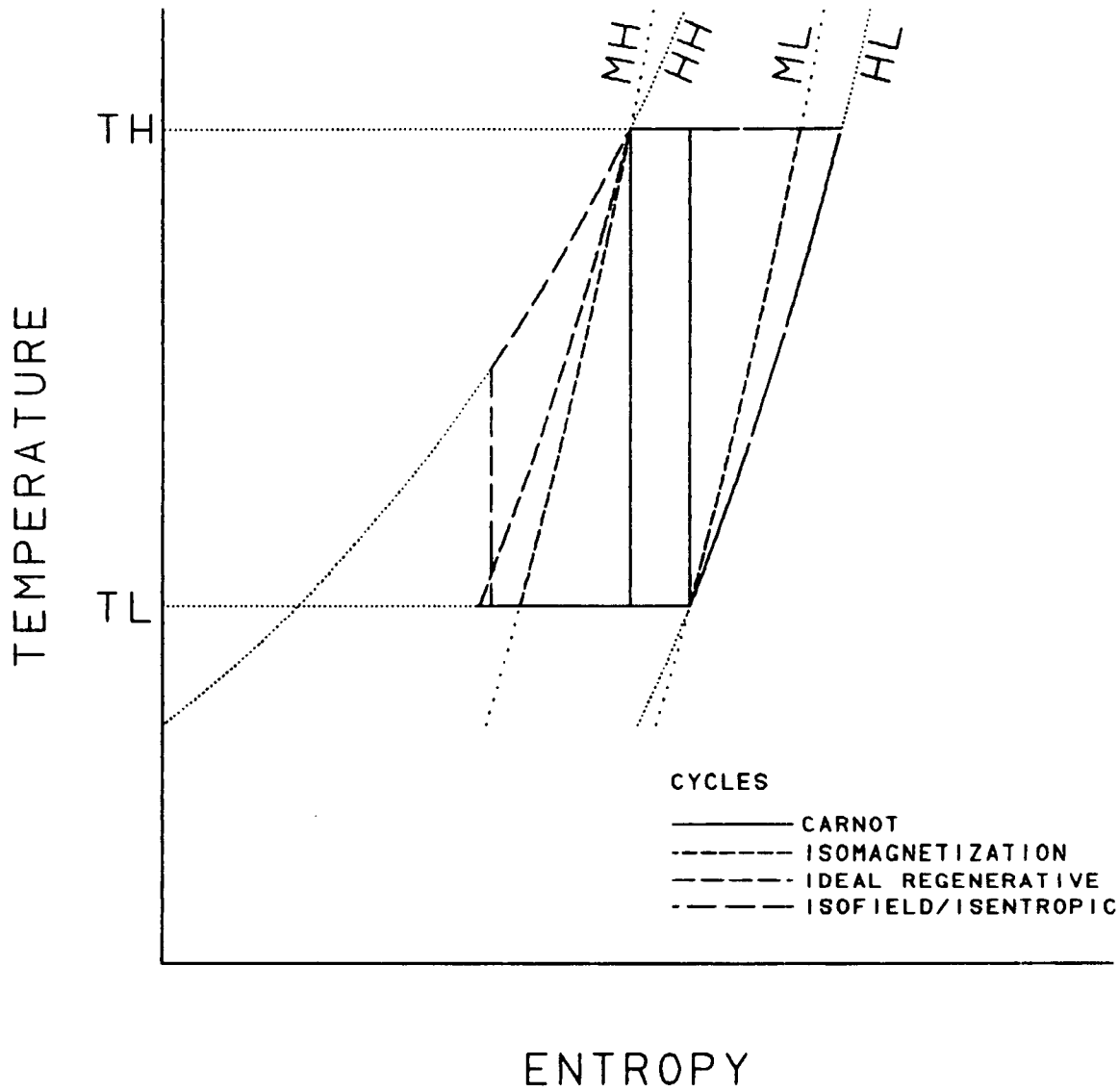

Fig. 3.2. T-s with constant magnetization and field lines; Carnot, constant magnetization, ideal regenerative, and constant field cycles.

ORNL-DWG 90-11719

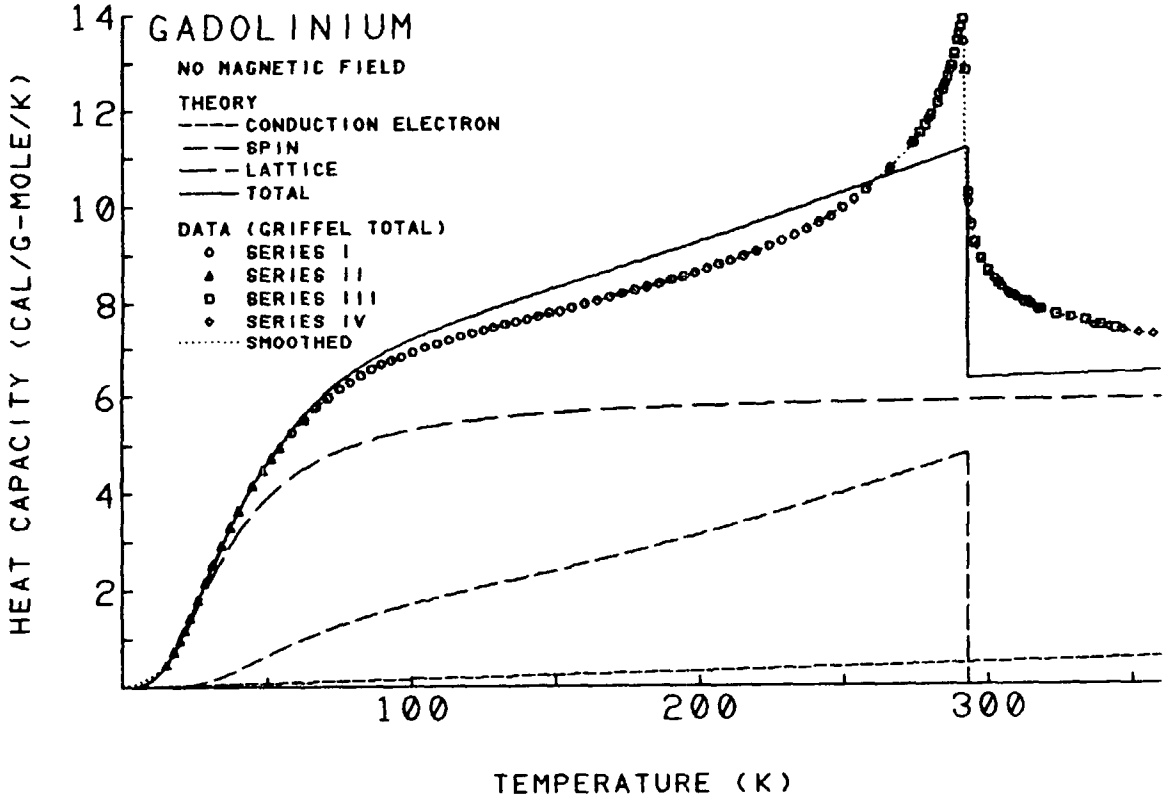

Fig. 3.3. c-T for zero field; lattice, electron, and spin components from molecular field theory; Griffel data.

ORNL-DWG 90-11720

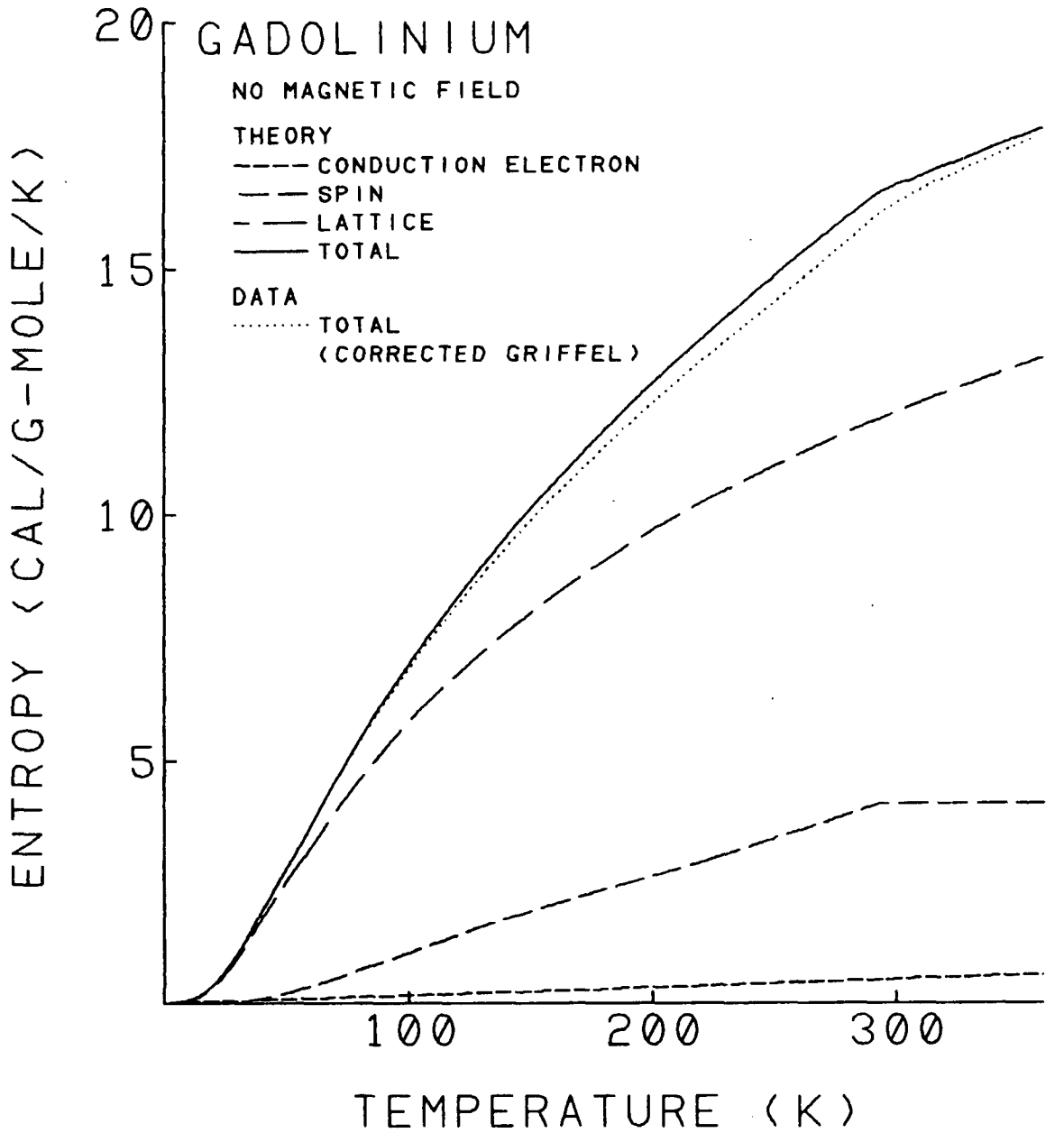

Fig. 3.4. T-s theory; integrated Griffel data from molecular field (corrected).

ORNL-DWG 90-11721

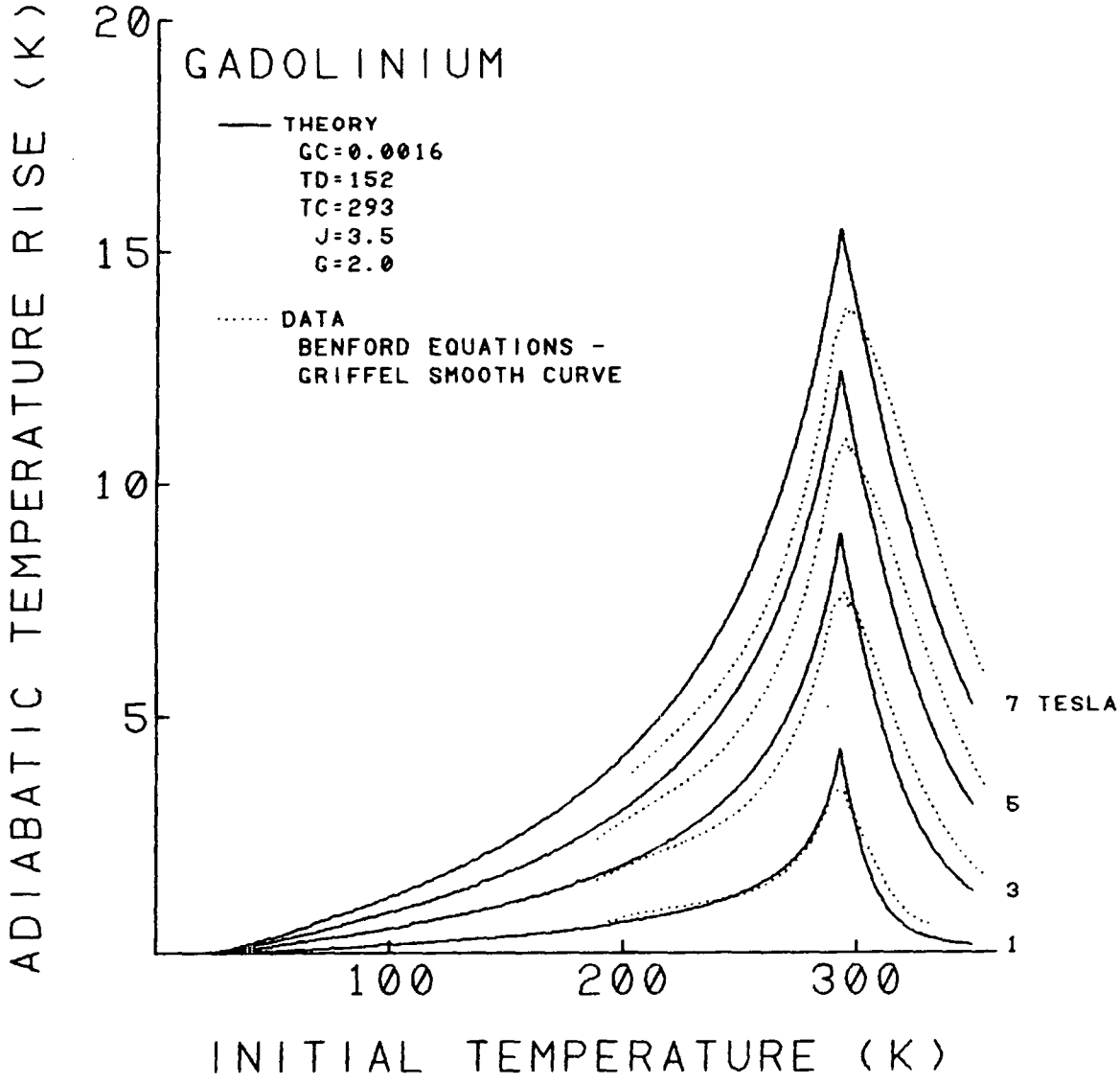

Fig. 3.5. Δ T-T for 1,3,5, and 7 T from molecular field theory; Benford data.

ORNL-DWG 90-11722

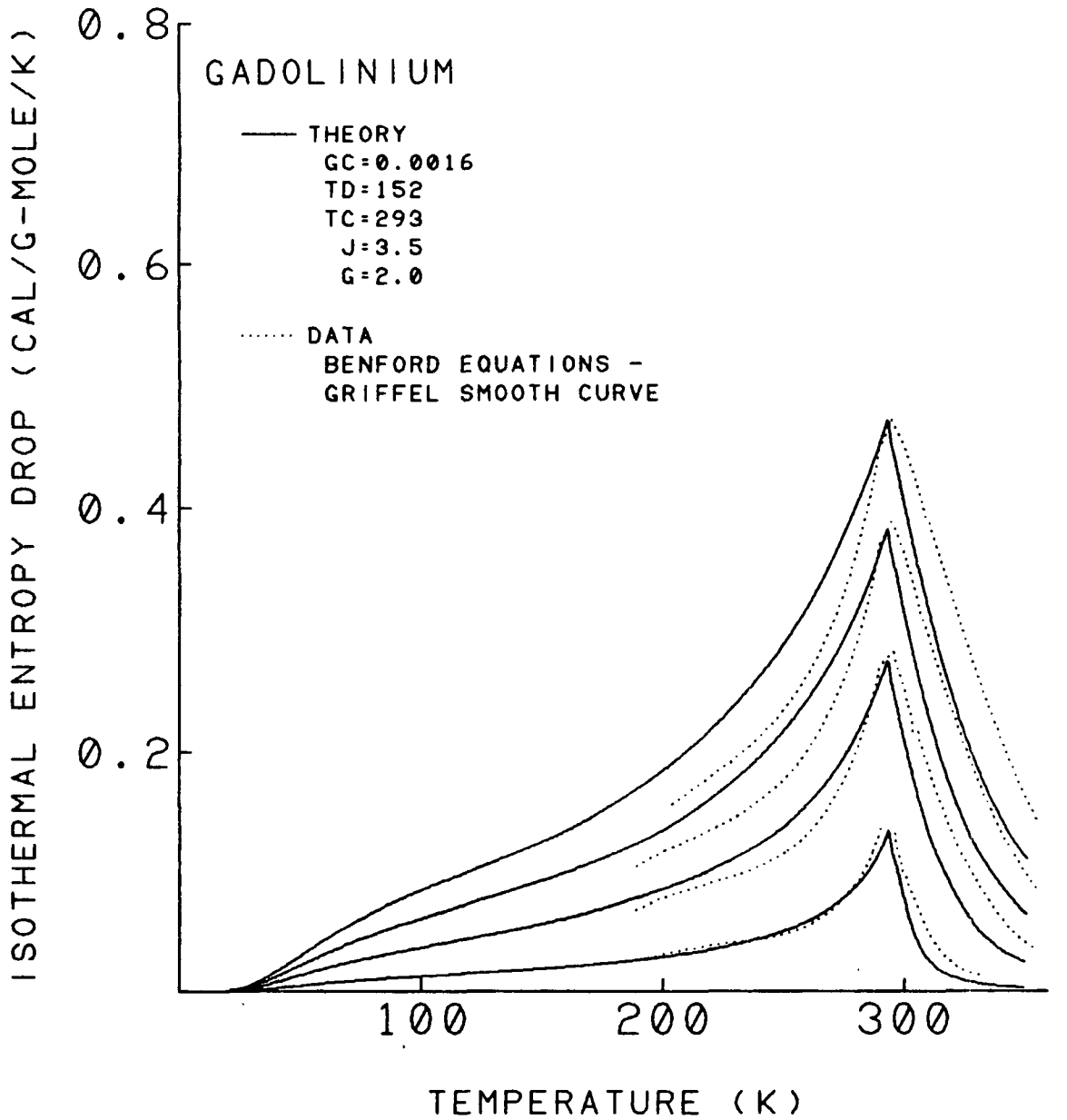

Fig. 3.6. Δ s-T for 1,3,5, and 7 T from molecular field theory; Benford data.

ORNL-DWG 90-11723

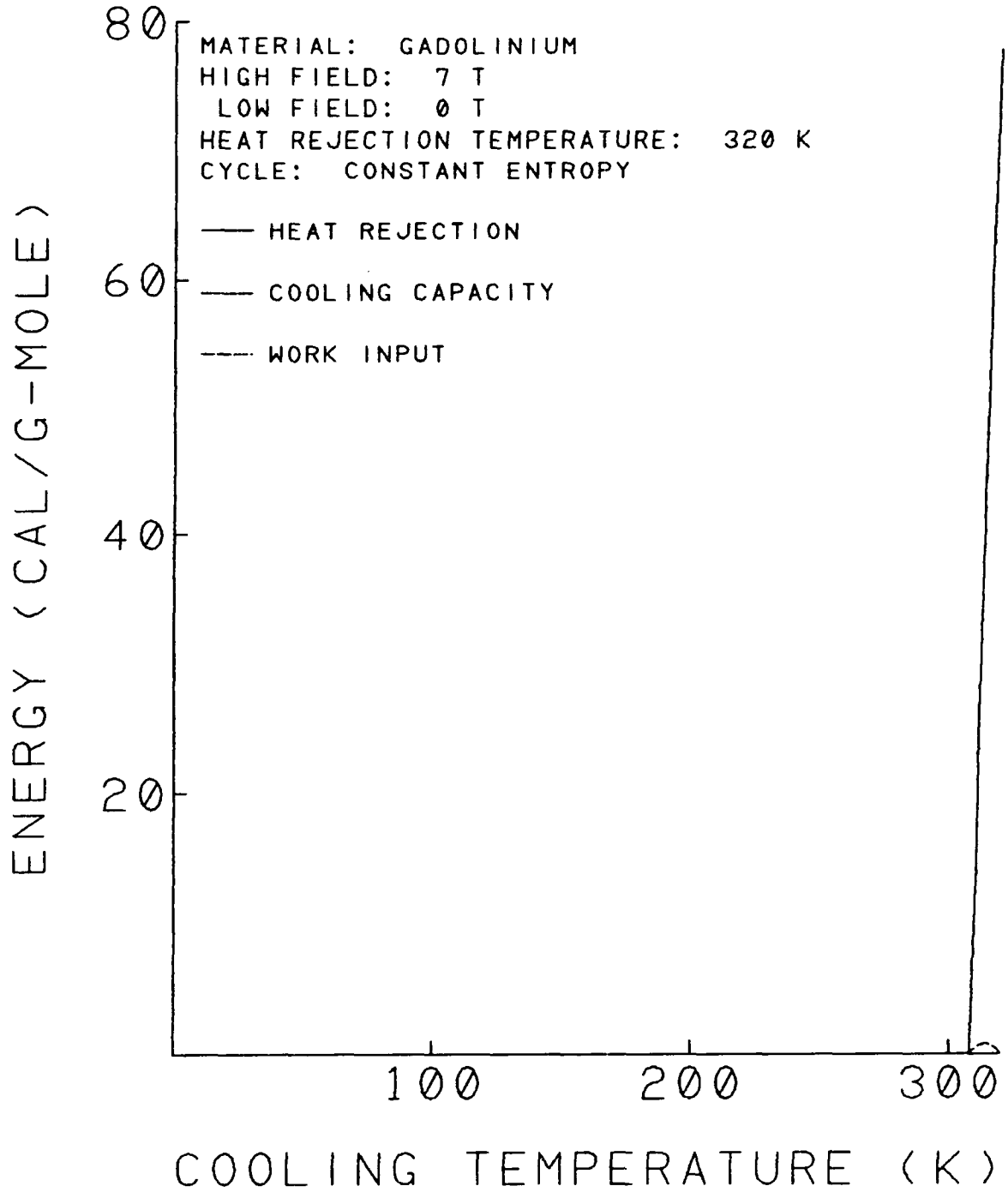

Fig. 3.7. Q_h,Q_c,W-T_1 for Carnot cycle.

ORNL-DWG 90-11724

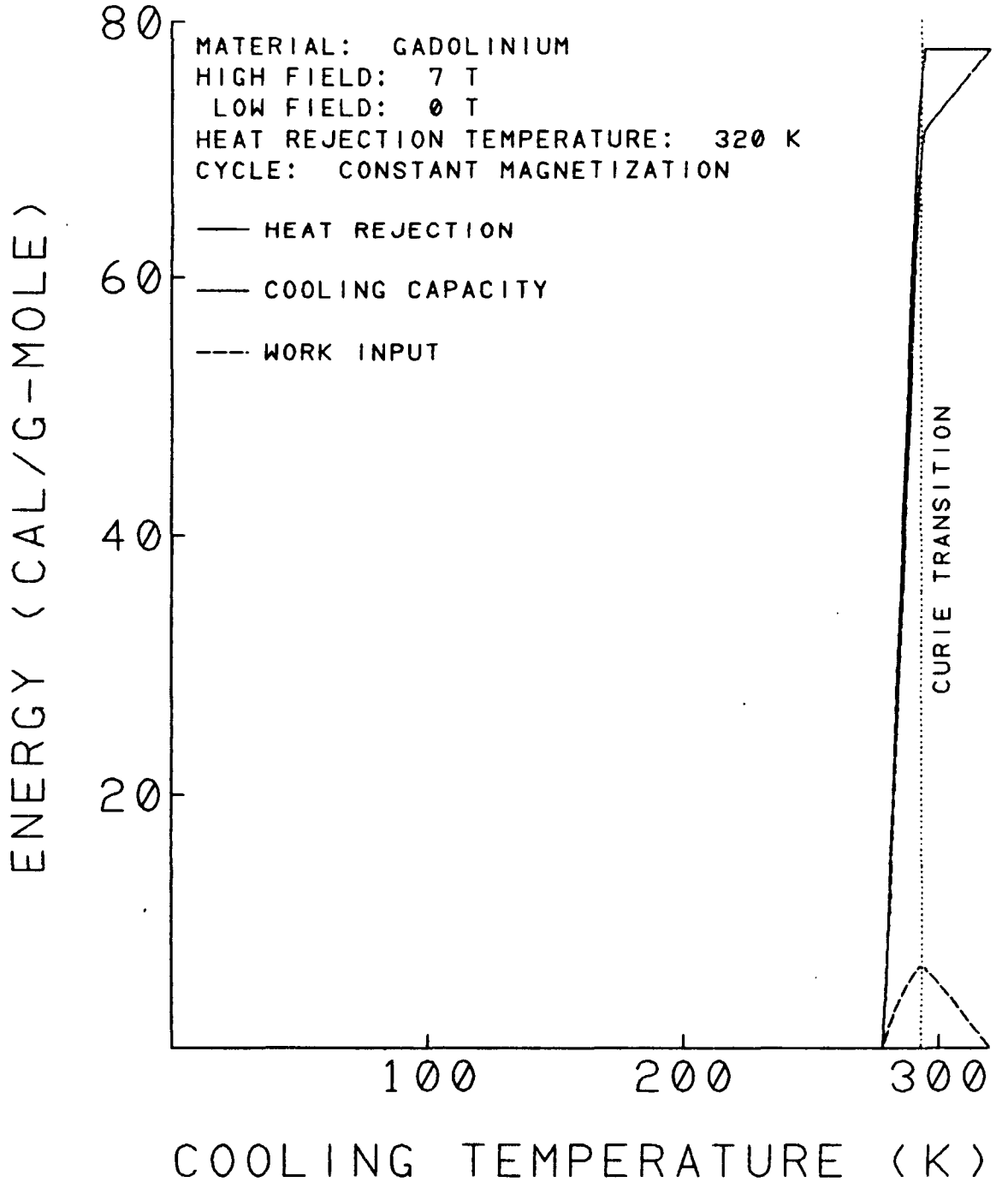

Fig. 3.8. Q_h,Q_c,W-T_1 for constant magnetization cycle.

ORNL-DWG 90-11725

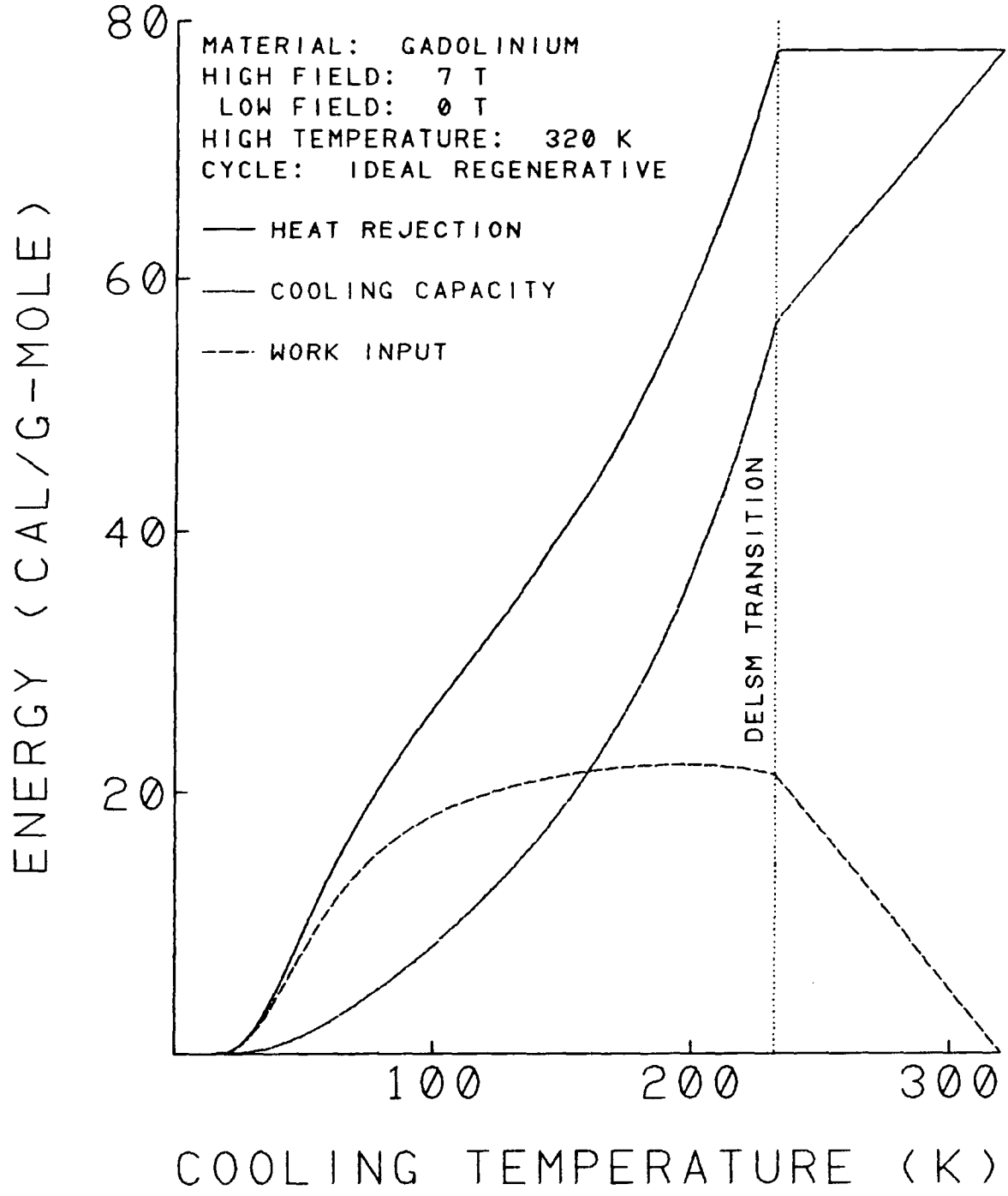

Fig. 3.9. Q_h,Q_cW-T_1 for ideal regenerative cycle.

ORNL-DWG 90-11726

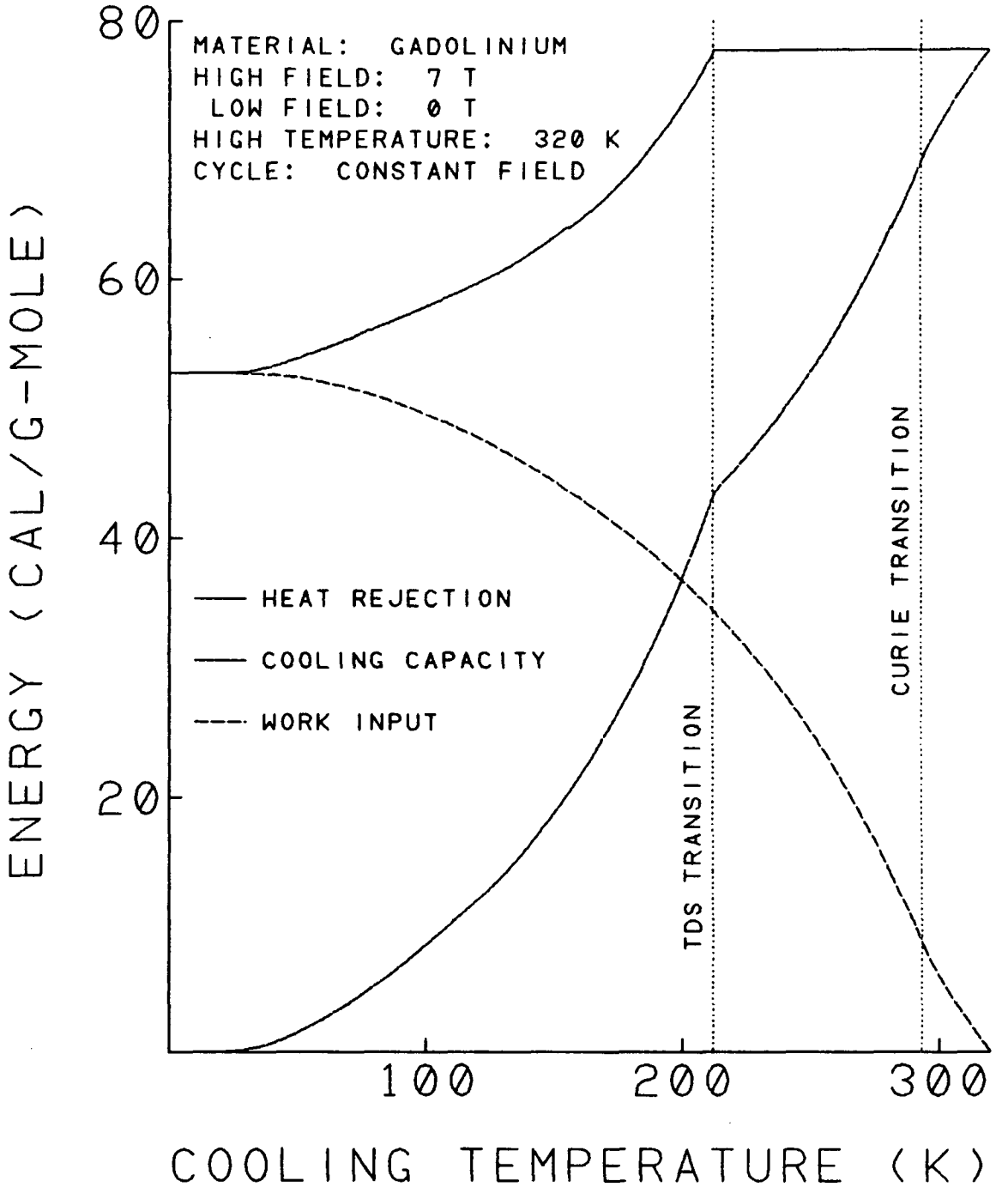

Fig. 3.10. Q_h,Q_c,W-T_1 for constant field cycle.

ORNL-DWG 90-11727

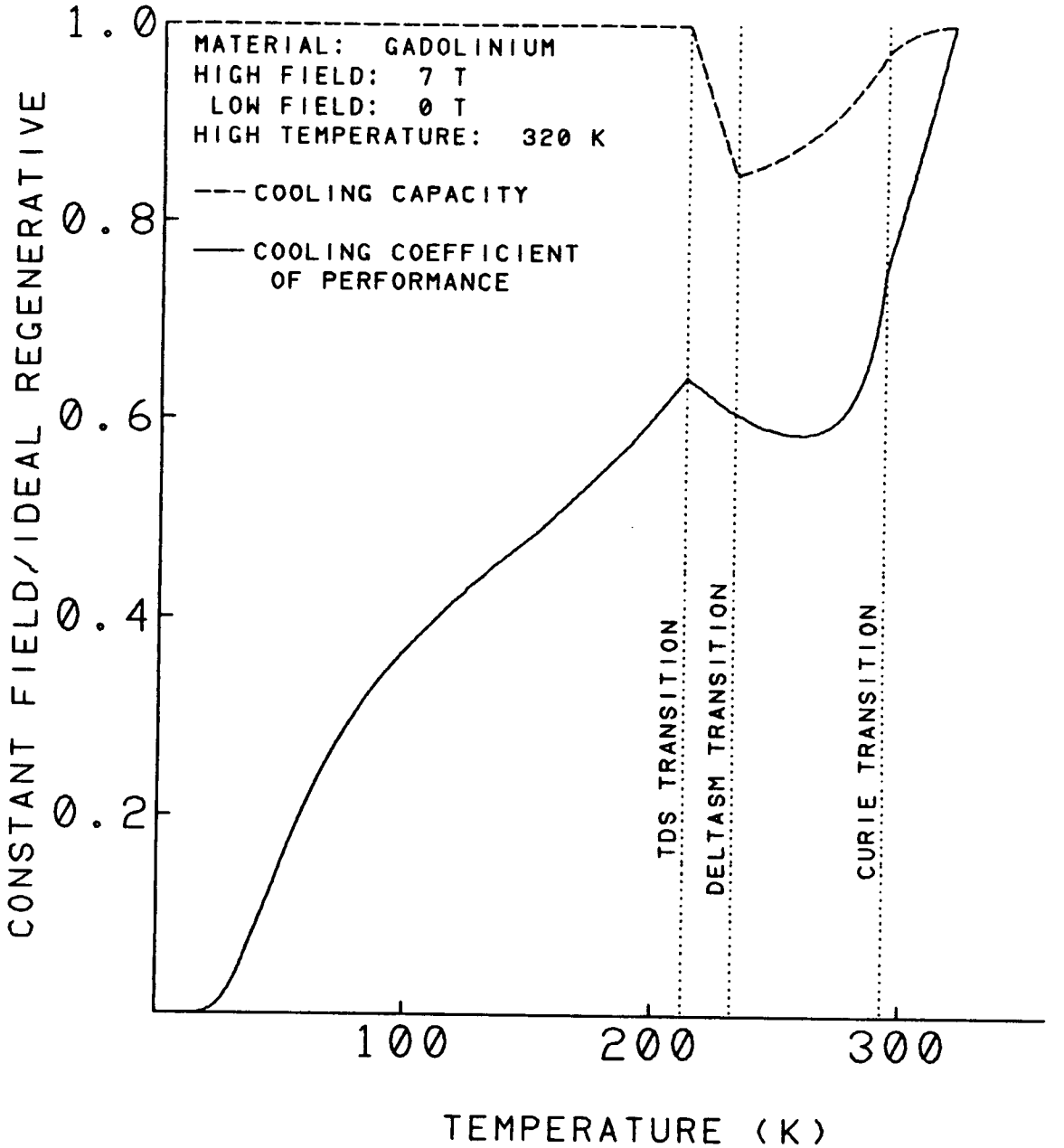

Fig. 3.11. Q_c and COP_c ratios-T_1.

ORNL-DWG 90-11728

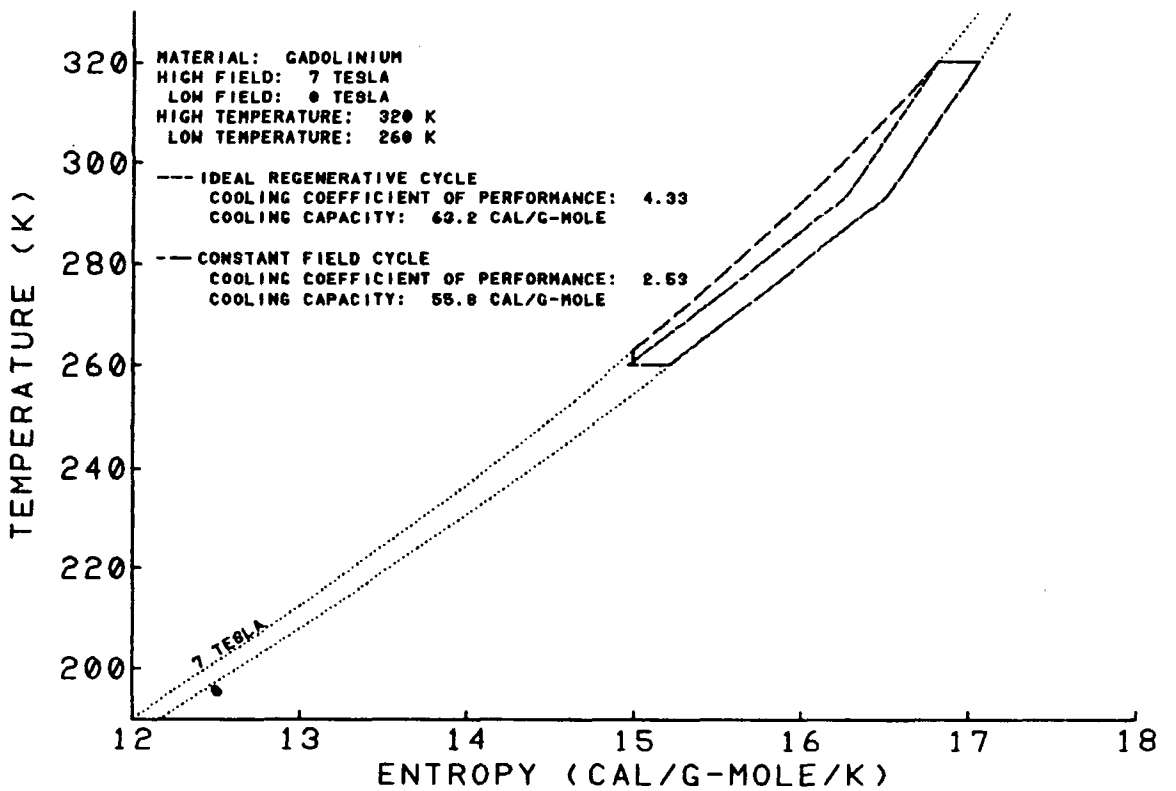

Fig. 3.12. T-s for T_1=260 K; ideal regenerative and constant field cycles.

ORNL-DWG 90-11729

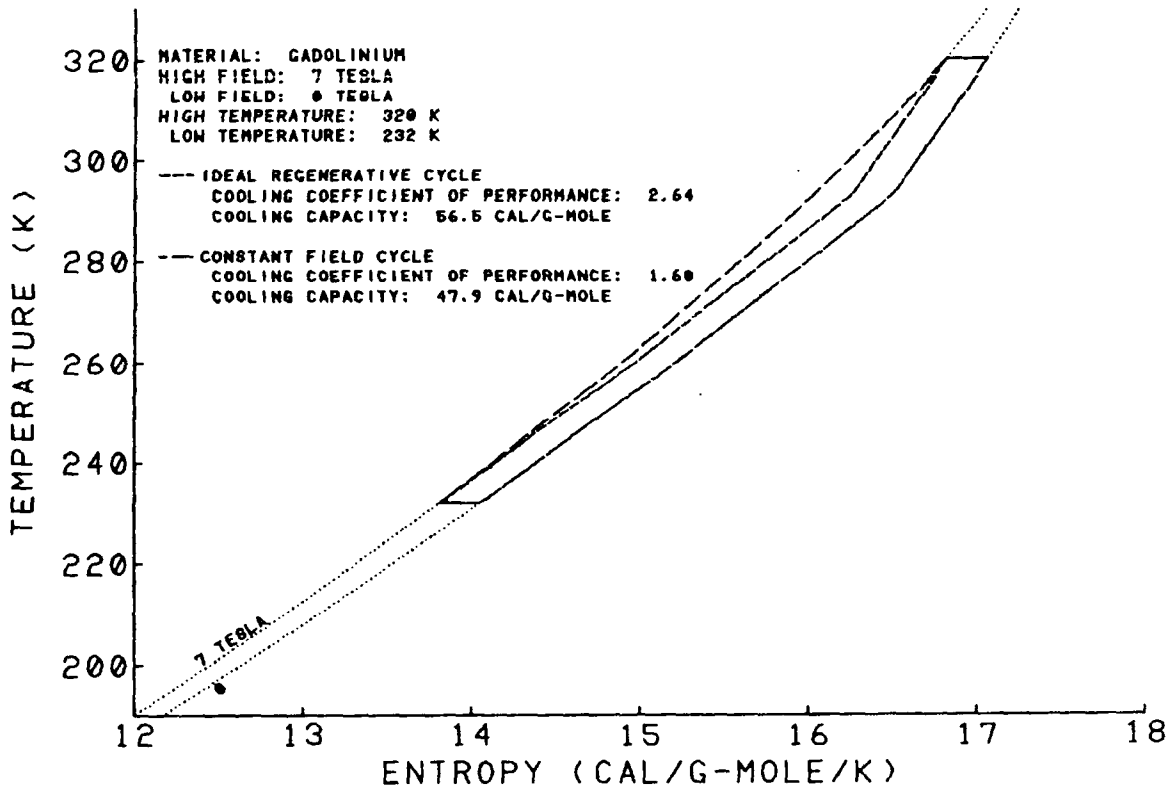

Fig. 3.13. T-s for T_1-232 K; ideal regenerative and constant field cycles.

ORNL-DWG 90-11730

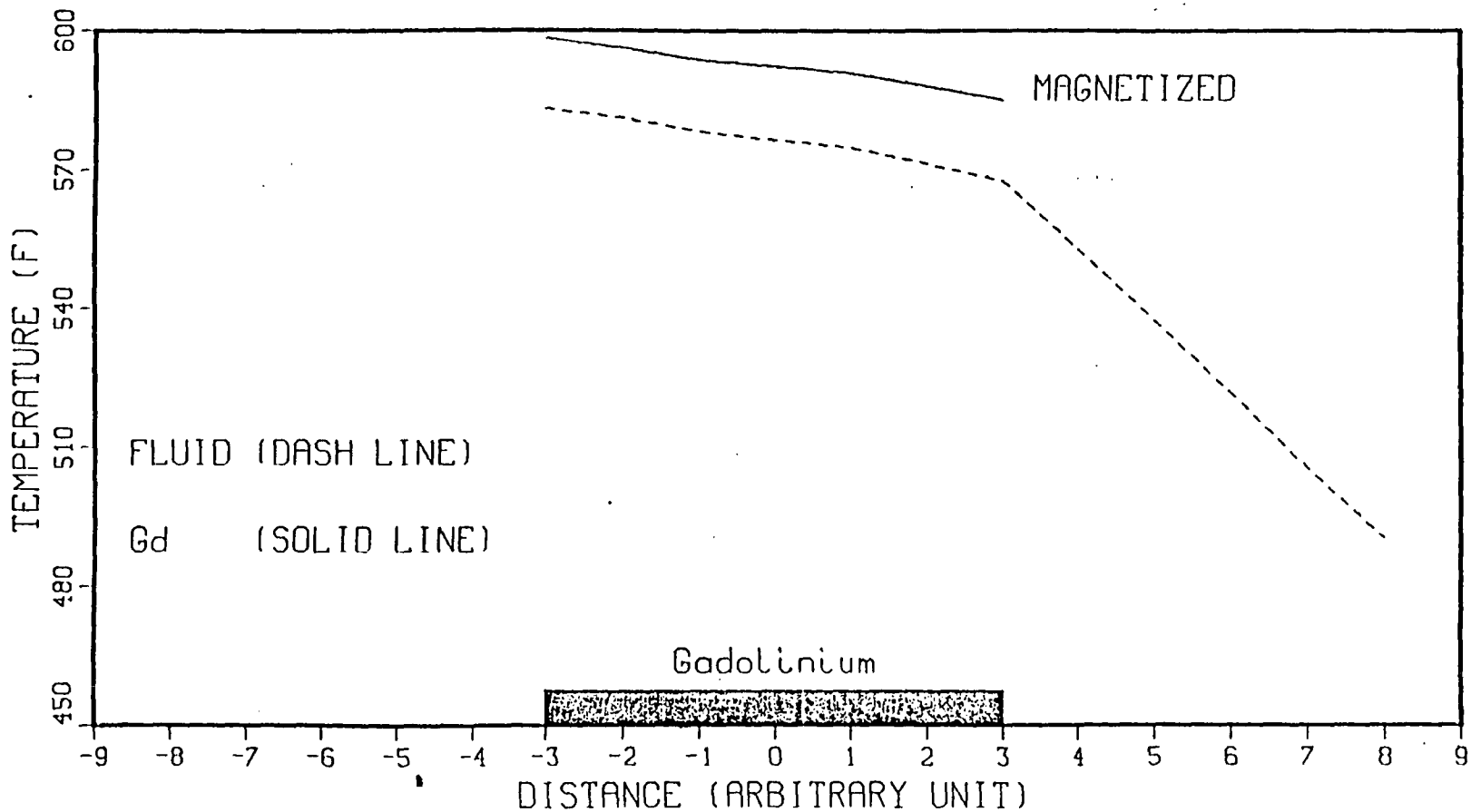

Fig. 4.1

ORNL-DWG 90-11758

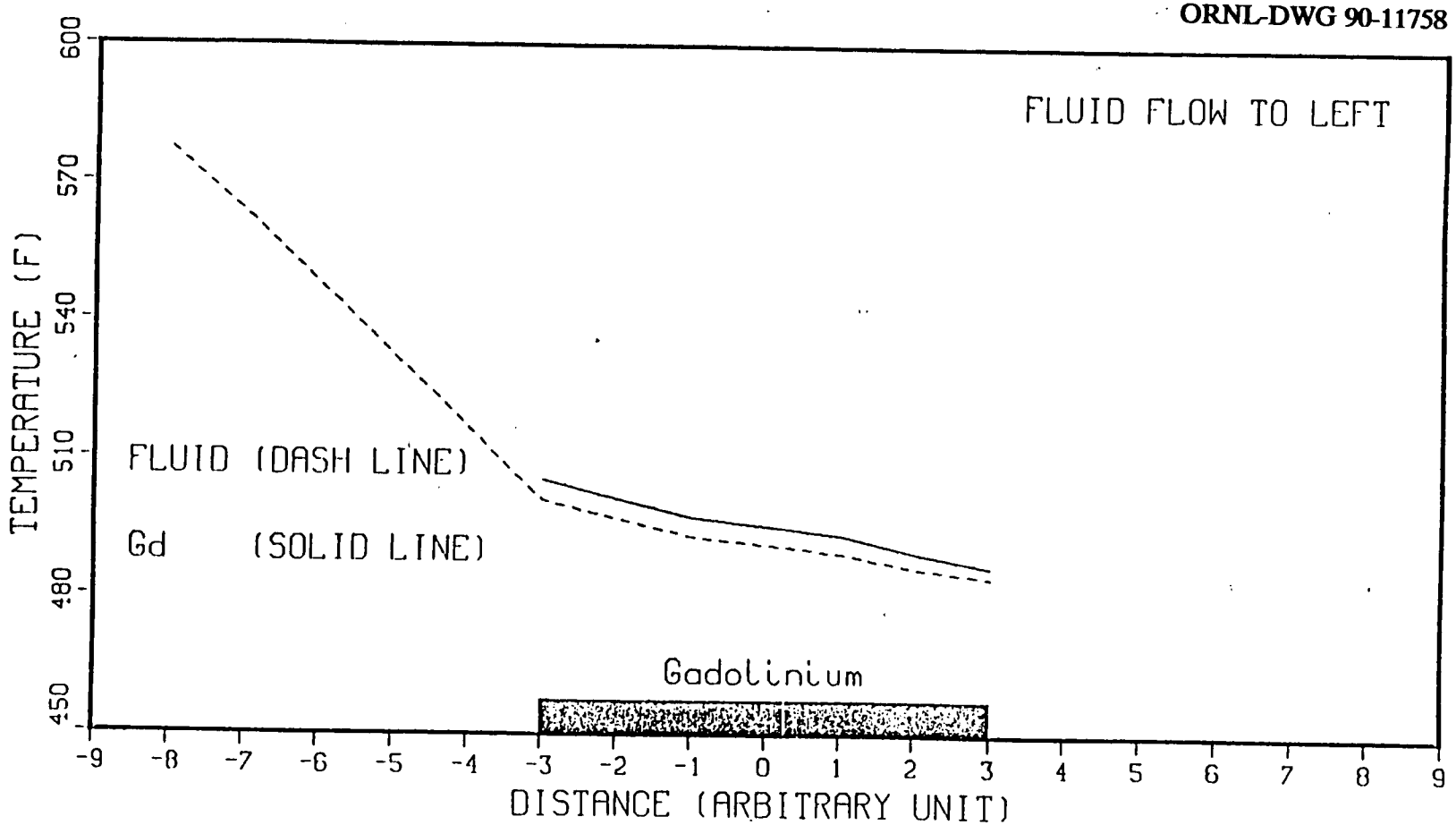

Fig. 4.2

ORNL-DWG 90-11759

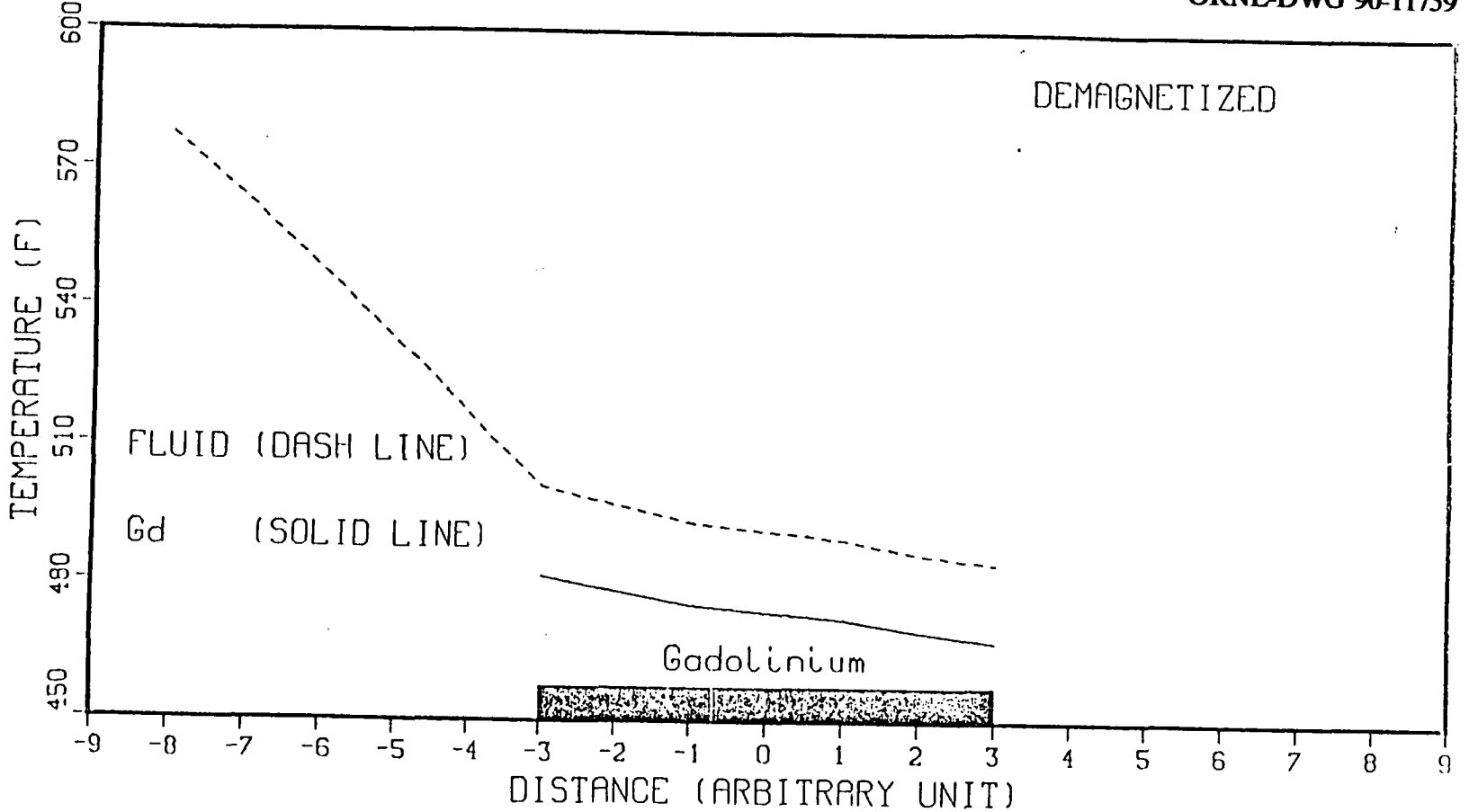

Fig. 4.3

ORNL-DWG 90-11760

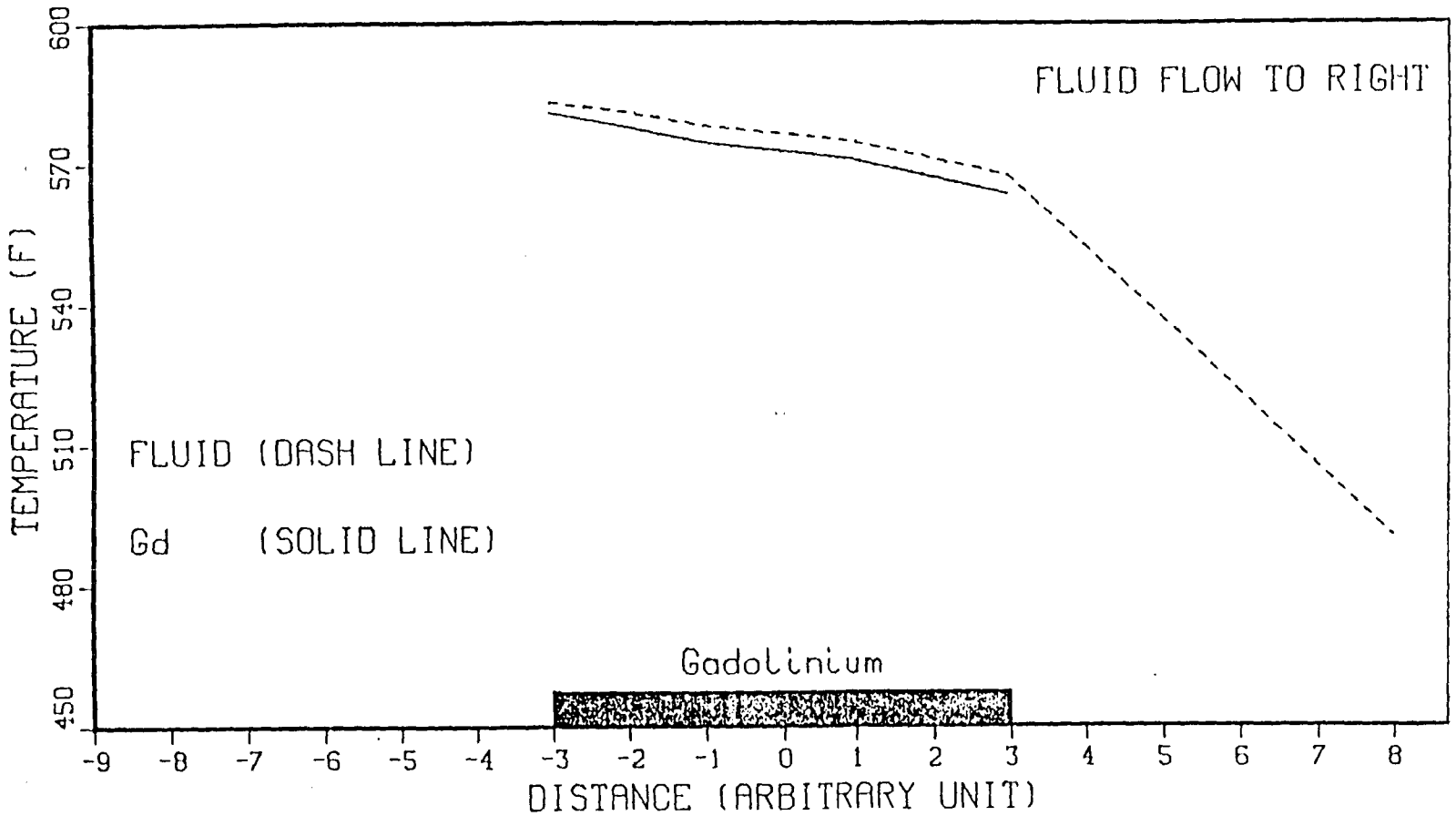

Fig. 4.4

APPENDIX A: Computer Code for Analysis of Heat Pump Cycles

```
C......THIS PROGRAM (STCYC2.FOR) IS USED TO THEORETICALLY CALCULATE
C......THE SPIN ENTROPY FOR CONSTANT MAGNETIZATION CYCLE
C......(STIRLING CYCLE) ANALYSIS.
C
C......"NAG" LIBRARY IS USED IN THIS PROGRAM FOR NUMERICAL INTEGRATION.
C
C........BC=BOLTZMANN'S CONSTANT(JOULE/K)
C........RMUB=BOHR MAGNETON (JOULE/TESLA)
C
      DOUBLE PRECISION C1,C2,C3,X,RM,T,H,BJ,SMR
      COMMON /PAM/RJN,H,T,C1,C2,C3
      DIMENSION HT(30)
      EXTERNAL F
      OPEN (UNIT=20,FILE='FOR20.DAT',STATUS='NEW')
      OPEN (UNIT=25,FILE='FOR25.DAT',STATUS='OLD')
       READ(25,*)RJN,TK,DTK
       WRITE(*,*)RJN,TK,DTK
       READ(25,*)MH,MT,(HT(I),I=1,MH)
       WRITE(20,*)MH,MT
      G=2.
      TC=291.76
      RMUB=9.27E-24
      BC=1.38E-23
      C1=(2*RJN+1.)/(2*RJN)
      C2=1./(2.*RJN)
      C3=3.*RJN/(RJN+1.)
      DO 40 I=1,MH
       H=G*RMUB*(RJN+1)*HT(I)/(3.*BC*TC)
       T=TK/TC
        DO 45 K=1,MT
        IF(T.GE.1..AND.H.EQ.0.)GO TO 60
        A=0.1
        X=C3/T*(H+1.)
        ESP=1.0E-05
        ETA=0.0
        IFAIL = 1
      CALL C05AJF(X,ESP,ETA,F,1000,IFAIL)
      RM=C1/DTANH(C1*X)-C2/DTANH(C2*X)
      SMR=DLOG(DSINH(C1*X)/DSINH(C2*X))-X*RM
      GO TO 70
60    SMR=DLOG(8.D0)
      RM=0.
70    CONTINUE
        TK2=T*TC
        SMR=SMR*1.987
      WRITE(20,50)HT(I),RM,TK2,SMR
        T=(TK+DTK*K)/TC
45      CONTINUE
       H=H+0.1
40     CONTINUE
50    FORMAT(1X,4E11.4)
      STOP
      END
      FUNCTION F(X)
      DOUBLE PRECISION C1,C2,C3,X,RM,T,H,BJ
      COMMON /PAM/RJN,H,T,C1,C2,C3
      BJ=C1/DTANH(C1*X)-C2/DTANH(C2*X)
      F=X-C3*(H+BJ)/T
      RETURN
      END
```

```
C...DATA FILE FOR25.DAT, INPUT FILE OF TOTEN.FOR AND STCYC2.FOR........
3.5 50. 0.5
2 543  0.0 7.0
```

```
C
C......THIS PROGRAM (TOTEN.FOR) IS USED TO CALCULATE THE THEORETICAL
C......VALUES OF TOTAL ENTROPY FOR Gd.
C
C......THIS PROGRAM NEEDS TO USE "NAG" LIBRARY FOR NUMERICAL INTEGRATION.
C
C........BC=BOLTZMANN'S CONSTANT(JOULE/K)
C........RMUB=BOHR MAGNETON (JOULE/TESLA)
C
      DOUBLE PRECISION C1,C2,C3,X,RM,T,H,BJ,SMR
      COMMON /PAM/RJN,H,T,C1,C2,C3
      DIMENSION HT(30)
      EXTERNAL F
      OPEN (UNIT=20,FILE='FOR20.DAT',STATUS='NEW')
      OPEN (UNIT=21,FILE='FOR21.DAT',STATUS='NEW')
      OPEN (UNIT=29,FILE='FOR29.DAT',STATUS='NEW')
      OPEN (UNIT=25,FILE='FOR25.DAT',STATUS='OLD')
       READ(25,*)RJN,TK,DTK
       WRITE(*,*)RJN,TK,DTK
       READ(25,*)MH,MT,(HT(I),I=1,MH)
       WRITE(20,*)MH,MT
      G=2.
      TC=291.76
      RMUB=9.27E-24
      BC=1.38E-23
      C1=(2*RJN+1.)/(2*RJN)
      C2=1./(2.*RJN)
      C3=3.*RJN/(RJN+1.)
      DO 40 I=1,MH
        H=G*RMUB*(RJN+1)*HT(I)/(3.*BC*TC)
        T=TK/TC
       DO 45 K=1,MT
         IF(T.GE.1..AND.H.EQ.0.)GO TO 60
         A=0.1
         X=C3/T*(H+1.)
         ESP=1.0E-05
         ETA=0.0
         IFAIL = 1
      CALL C05AJF(X,ESP,ETA,F,1000,IFAIL)
         RM=C1/DTANH(C1*X)-C2/DTANH(C2*X)
         SMR=DLOG(DSINH(C1*X)/DSINH(C2*X))-X*RM
      GO TO 70
60       SMR=DLOG(8.D0)
         rm=0.
70    CONTINUE
         CALL SL(T,SLR)
         SMR=SMR*1.987
         SLR=SLR*1.987
         TK2=T*TC
         SE=2.3E-03*TK2
      SLT=SMR+SLR+SE
      WRITE(20,50)HT(I),RM,TK2,SLT,SMR,SLR
      WRITE(29,*)TK2,SLT
         IF(TK2.GE.284. .AND. TK2.LE.300. .AND. HT(I).EQ.7.) THEN
         RG1=SLT
         CM1=3.74+SLR +SE
         CM2=4.0+SLR +SE
      WRITE(21,50)TK2,RG1,CM1,CM2
         END IF
      T=(TK+DTK*K)/TC
```

APPENDIX B: Example of Loss Calculations

LOSS CALCULATION

The loss calculation here is calculated by Kirol et al. [ref. 13 of Section 2]. Their calculation is based on the second law of thermodynamics. They have calculated five different losses:

1. loss due to heat transfer,
2. loss due to differences in specific heat,
3. loss due to pump work,
4. loss due to variable specific heat, and
5. loss due to differences in specific heat plus pump work.

Since the methods used to calculate each loss are very similar to each other, an example using loss no. 1 (due to heat transfer) is provided below to show the procedure of calculation.

1. Loss Due to Heat Transfer

This calculation is to estimate reduction in efficiency due to heat transfer temperature drops alone.

1.1 Assumptions

- Core material: gadolinium (Gd)
- Specific heat: 230 J/Kg-K average
- Field strength: 0-9 T
- Entropy change: 14.4 J/Kg-K at Curie Point (293 K). Average entropy change is assumed to be 7 J/Kg-K.
- Heat pump operating temperature span: 56 K (100°F)
- Frequency: 1 cycle/s
- Convective heat transfer coefficient between Gd and fluid: 6,300 W/m^2-K
- Working material area: 5 m^2
- Cycle operated around the Curie Point

1.2 Required Heat Transfer

$$Q = 230 \times 56 = 12{,}880 \text{ W/Kg}$$

1.3 Heat Transfer Temperature Drop

$$\Delta T = \frac{12{,}880}{5 \times 63{,}000} = 0.041\text{K}$$

1.4 Temperatures (from Fig. 1)

$$T_1 = T_2 = 293 + 28 = 321 \text{ K}$$
$$T_6 = T_2 - 0.041 = 320.959 \text{ K}$$
$$T_4 = T_5 = 293 - 28 = 265 \text{ K}$$
$$T_3 = T_4 + 0.041 = 265.041 \text{ K}$$

1.5 Entropy Calculation for Constant Specific Heat and Field

$$TdS = C_p\ (T_2 - T_3)(S_2 - S_3)/\ln(T_2/T_3)$$

Letting $S_4 = 0.0$ and $S_3 = 0.0$

then $S_2 = 44.058$
$S_1 = S_2 + 7$
$S_5 = S_1 - C_P \ln(T_C/T_5) = 6.99$

1.6 Heat Flows and Efficiency

$$Q_H = T_2(S_1 - S_2) = 2{,}247\ J$$

$$Q_L = T_4(S_5 - S_4) = 1{,}852\ J$$

$$COP = \frac{Q_H}{Q_H - Q_L} = 5.689$$

$$Eff = \frac{COP\,(T_H - T_L)}{T_H} = 99.2\%$$

APPENDIX C: Transient Heat Transfer Model for a Magnetic Heat Pump

```
C
C       THIS PROGRAM IS MHSYS.1.  IT IS FOR THE SIMULATION OF THE MH
C       SYSTEM TO BE BUILT.  THE EQUATIONS WERE FOR COUPLED TRANSIENT
C       HEAT TRANSFER OF FLUID AND GADILIUM.
C
C
        IMPLICIT REAL*8(A-H,O-Z)
        DIMENSION T(60,20),U(60,20),TE(60),DELTA(20),UD(60,20),TD(60,20)
        DIMENSION TK(60,20),UK(60,20)
C
C       READ IN THE CONSTANTS
C
        READ(20,10)CF,CS,ALPHA,VF,RHOF,RHOS,TI
        READ(20,11)H,DKS,DI,DX,DT,M,N,DL
10      FORMAT(7F10.3)
11      FORMAT(2F10.2,F10.4,2F10.2,2I5,F10.2)
        PI=3.1415927D0
        A=PI*DI*DI/4.0D0/144.0D0
C
C       SETUP THE CONSTANTS FOR TEMPERATURE CALCULATION.
C
C       FLUID TEMPERATURE CONSTANTS
C
        C2 = VF*DT/3600.0D0/ALPHA/DX*12.0D0
        C3 = 2.0*H*DL*DT/3600.0D0/ALPHA/RHOF/CF/A
        C1 = 1.0D0 -C2-C3
C
C       GD CORE TEMPERATURE CONSTANTS
C
        C5 = 2.0D0*H*DL*DT/3600.0D0/(1.0D0-ALPHA)/RHOS/A/CS
        C6 = DKS*DT/3600.0D0/RHOS/CS/DX/DX*144.0D0
        C4 = 1.0D0-C5-2.0D0*C6
        WRITE(6,600)C1,C2,C3,C4,C5,C6
600     FORMAT(2X,6F9.4)
C
C       READ IN INITIAL FLUID AND GD TEMPERATURE, ASSUMED TO BE UNIFORM
C
        DO 21 J=1,N
        T(1,J)=TI
        U(1,J)=TI
        UK(1,J)=TI/1.8D0
        TK(1,J)=TI/1.8D0
21      CONTINUE
        DO 25 I=1,M
25      TE(I) = TI
        MM = 1
C
C       CALCULATE THE TEMPERATURE LIFT, OR FALL, OF GD CORE WHEN
C       MAGNETIZED, OR DE-MAGNETIZED
C
140     CONTINUE
        IF(MM .EQ.1)GO TO 160
        DO 170 J=1,N
        U(1,J) = UD(M,J)
        T(1,J) = TD(M,J)
        UK(1,J)=UD(M,J)/1.8D0
        TK(1,J)=TD(M,J)/1.8D0
170     CONTINUE
160     DO 40 J=1,N
        IF(UK(1,J) .GE. 200.0D0 .AND. UK(1,J) .LE. 250.0D0)
```

```
     *  DELTA(J)=6.32D-4*UK(1,J)**2 - 2.146D-1*UK(1,J) + 21.83D0
        IF(UK(1,J) .GT. 250.0D0 .AND. UK(1,J) .LE. 293.0D0)DELTA(J)=
     *  2.5766D-3*UK(1,J)**2 - 1.2179445D0*UK(1,J) + 151.12708D0
        IF(UK(1,J) .GT. 293.0D0 .AND. UK(1,J) .LE. 350.0D0)DELTA(J)=
     *  1.380117D-3*UK(1,J)**2 - 1.0660117D0*UK(1,J) + 209.33D0
        DELTA(J)=DELTA(J)*1.8D0
        UK(1,J)=UK(1,J)*1.8D0
        IF(DMOD(DBLE(MM),DBLE(2))+1 .EQ. 2)U(1,J) = U(1,J) + DELTA(J)
        IF(DMOD(DBLE(MM),DBLE(2))+1 .NE. 2)U(1,J) = U(1,J) - DELTA(J)
        WRITE(6,500)J,DELTA(J),UK(1,J),U(1,J)
500     FORMAT(2X,I3,3F10.2)
40      CONTINUE
C
C       START MARCHING OF U & T IN TIME "t" AND ALONG GD CORE "X"
C
        DO 45 I=1,M-1
        DO 50 J=1,N
        IF(J.NE.1)GO TO 52
        T(I+1,J) = C1*T(I,J)+C2*TE(I)+C3*U(I,J)
        U(I+1,J) = C4*U(I,J)+C5*T(I,J)+C6*2.0D0*U(I,J+1)
        IF(J.EQ.1)GO TO 50
52      T(I+1,J) = C1*T(I,J)+C2*T(I,J-1)+C3*U(I,J)
        IF(J .EQ. N) GO TO 54
        U(I+1,J) =C4*U(I,J) + C5*T(I,J) + C6*(U(I,J+1) + U(I,J-1))
        GO TO 50
54      U(I+1,J) =C4*U(I,J) + C5*T(I,J) + C6*2.0D0*U(I,J-1)
50      CONTINUE
        WRITE (6,90) MM,I,J-1,U(I,J-1),T(I,J-1),DELTA(J-1)
100     CONTINUE
90      FORMAT(2X,3I3,2X,3F10.3)
C56      IF(U(I+1,J) .GT. 630.0D0 .OR. U(I+1,J) .LT.360.0D0)GO TO 125
45      CONTINUE
        DO 750 J=1,N
750     WRITE(6,760)M,MM,J,U(M,J),T(M,J)
760     FORMAT(2X,3I3,2F10.2)
C
C       STORE FLUID TEMPERATURE OUT OF GD CORE
C
        DO 60 I = 1,M
        LL=DBLE(M)-DBLE(I)+DBLE(1)
60      TE(LL) = T(I,N)
        DO 770 I = 1,M,10
770     WRITE(6,660)I,TE(I),T(I,N)
660     FORMAT(10X,I3,2F10.3)
C
C
        MM=MM+1
        IF(MM .GT. 51)GO TO 130
C
C       START REVERSING THE FLOW & CHANGE THE MAGNETIOC PROCESS
C
        DO 70 J=1,N
C
C       ADD THE NEXT FOUR LINES TO ASSUME THE EVEN OUT OF FLUID AND
C       MAGNETIC CORE TEMPERATURE DURING THE GD CORE "STOP" PERIOD
C
        T(M,J)=(RHOF*CF*T(M,J)+RHOS*CS*U(M,J))/(RHOF*CF+RHOS*CS)
        U(M,J)=T(M,J)
        TD(M,N-J+1) = T(M,J)
        UD(M,N-J+1) = U(M,J)
```

```
70      CONTINUE
        I=1
        GO TO 140
C125     WRITE(6,150)
C150     FORMAT(' U IS EITHER LARGER THAN 630.0, OR SMALLER THAN 360.0')
130     STOP
        END
```

```
45        CONTINUE
        H=H+0.1
40      CONTINUE
50    FORMAT(1X,6E11.4)
      STOP
      END
      FUNCTION F(X)
      DOUBLE PRECISION C1,C2,C3,X,RM,T,H,BJ
      COMMON /PAM/RJN,H,T,C1,C2,C3
      BJ=C1/DTANH(C1*X)-C2/DTANH(C2*X)
      F=X-C3*(H+BJ)/T
      RETURN
      END
      SUBROUTINE SL(TC,ANS)
        IMPLICIT REAL*8(a-h,o-z)
        INTEGER*4 NPTS,IFAIL,NOUT
        EXTERNAL FA
       NLIMIT=0
       EPSR=1.0E-05
       IFAIL=1
       T1=TC*291.76/152.
         YA=0.
         YB=1./T1
         ANS=D01AHF(YA,YB,EPSR,N,RELERR,FA,NLIMIT,
     1     ifail)
       ANS=ANS*12.*T1**3-3*DLOG(1.-DEXP(-1./T1))
       RETURN
       END
        real function fa(x)
        implicit real*8(a-h,o-z)
      FA=X**3/(DEXP(X)-1.)
          return
          end
```

```
C.....THIS PROGRAM (PLOTWQ1.FOR) IS USED TO CALCUATE AND PLOT
C.....THE HEAT REJECTION, COOLING CAPACITY AND WORK INPUT
C.....FOR IDEAL REGENERATIVE CYCLE.
C.....PART OF INPUT  FILE OF THIS PROGRAM IS THE OUTPUT OF " TOTEN.FOR ".
C....."DISSPLA" IS USED FOR PLOTTING.
      DIMENSION T(400),QH(400),QL(400),W(400),QHP(2),QLP(2),WP(2),TP(2)
      DIMENSION ST0(400),ST7(400)
      CHARACTER YTITLE*100,XTITLE*100,TITLE*100
      CHARACTER CYNAME*100,MATNAME*100
      INTEGER HFIELD,LFIELD,HT
       OPEN (UNIT=20,FILE='PLOTWQ1.DAT',STATUS='OLD')
       OPEN (UNIT=25,FILE='FOR99.DAT',STATUS='NEW')
        READ(20,*)HFIELD,LFIELD,HT
        READ(20,*)S1,S2,S3,S4,S5,S6
        READ(20,*)TITLE
        READ(20,*)XTITLE
        READ(20,*)YTITLE
        READ(20,*)CYNAME
        READ(20,*)MATNAME
        READ(20,*)RX0,RX1,RX2,RX3,RX4,RX5,RX6,RX7
        READ(20,*)RY0,RY1,RY2,RY3,RY4,RY5,RY6,RY7
        READ(20,*)TP(1),TP(2),QHP(1),QHP(2),QLP(1),QLP(2),WP(1),WP(2)
        READ(20,*)M
      DO 40 I=1,M
40       READ(20,*)T(I),ST0(I)
      DO 50 I=1,M
50       READ(20,*)T7,ST7(I)
         DSTH=ST0(M)-ST7(M)
      DO 70 I=1,M
         DST=ST0(I)-ST7(I)
      IF(DSTH.LE.DST)THEN
         QH(I)=HT*DSTH
         QL(I)=T(I)*DSTH
         W(I)=QH(I)-QL(I)
        END IF
      IF(DSTH.GT.DST)THEN
         QH(I)=HT*DST
         QL(I)=T(I)*DST
         W(I)=QH(I)-QL(I)
        END IF
      IF(W(I).GT.0.)COP=QL(I)/W(I)
        WRITE(25,*)T(I),QL(I),COP
70    CONTINUE
9     FORMAT(I6,10E10.3)
       CALL COMPRS
       CALL PAGE(11.,8.5)
       CALL AREA2D(6.0,7.0)
       CALL HEADIN(% REF(TITLE),100,1.5,1)
       CALL XNAME(% REF(XTITLE),100)
       CALL YNAME(% REF(YTITLE),100)
       CALL INTAXS
       CALL FRAME
       CALL THKFRM(.01)
       CALL GRAF(S1,S2,S3,S4,S5,S6)
       CALL CURVE(T,QH,M,0)
       CALL CURVE(TP,QHP,2,0)
       CALL DASH
       CALL CURVE(T,QL,M,0)
       CALL CURVE(TP,QLP,2,0)
       CALL DOT(T,W,M,0)
       CALL CURVE(T,W,M,0)
```

```
CALL CURVE(TP,WP,2,0)
CALL RLMESS (% REF(MATNAME),100,RX0,RY0)
CALL RLMESS (% REF(CYNAME),100,RX1,RY1)
CALL RLMESS ('HIGH FIELD:  $',100,RX2,RY2)
CALL RLINT(HFIELD,'ABUT','ABUT')
CALL RLMESS ('LOW FIELD:   $',100,RX3,RY3)
CALL RLINT (LFIELD,'ABUT','ABUT')
CALL RLMESS ('HIGH TEMPERATURE:   $',100,RX4,RY4)
CALL RLINT (HT,'ABUT','ABUT')
CALL RLMESS ('HEAT REJECTION$',100,RX5,RY5)
CALL RLMESS ('COOLING CAPACITY$',100,RX6,RY6)
CALL RLMESS ('WORK INPUT$',100,RX7,RY7)
CALL ENDPL(0)
CALL DONEPL
STOP
END
```

```
C....PARTIAL LISTING OF DATA FILE "PLOTWQ1.DAT", INPUT FILE OF PLOTWQ1.FOR
7 0 320
0. 80. 320. 0. 20. 80.
' $'
'COOLING TEMPERATURE (K)$'
'ENERGY (Cal./g-mole)$'
'Cycle: Ideal rEGENERATIVE$'
'Material: Gd$'
10. 10. 10. 10. 10. 35. 35. 35.
78. 74. 70. 66. 62. 58. 54. 50.
10. 30. 58. 58. 54. 54. 50. 50.
271
 0.0000E+00 0.9939E+00 0.5000E+02 0.2828E+01 0.2063E+00 0.2506E+01
 0.0000E+00 0.9934E+00 0.5100E+02 0.2921E+01 0.2198E+00 0.2584E+01
 0.0000E+00 0.9929E+00 0.5200E+02 0.3015E+01 0.2335E+00 0.2662E+01
 0.0000E+00 0.9923E+00 0.5300E+02 0.3109E+01 0.2475E+00 0.2739E+01
 0.0000E+00 0.9917E+00 0.5400E+02 0.3202E+01 0.2618E+00 0.2816E+01
 0.0000E+00 0.9912E+00 0.5500E+02 0.3295E+01 0.2763E+00 0.2892E+01
 0.0000E+00 0.9905E+00 0.5600E+02 0.3388E+01 0.2911E+00 0.2968E+01
 0.0000E+00 0.9899E+00 0.5700E+02 0.3481E+01 0.3061E+00 0.3044E+01
 0.0000E+00 0.9893E+00 0.5800E+02 0.3573E+01 0.3212E+00 0.3118E+01
 0.0000E+00 0.9886E+00 0.5900E+02 0.3665E+01 0.3366E+00 0.3193E+01
 0.0000E+00 0.9879E+00 0.6000E+02 0.3757E+01 0.3522E+00 0.3267E+01
 0.0000E+00 0.9872E+00 0.6100E+02 0.3848E+01 0.3679E+00 0.3340E+01
 0.0000E+00 0.9864E+00 0.6200E+02 0.3939E+01 0.3838E+00 0.3413E+01
 0.0000E+00 0.9857E+00 0.6300E+02 0.4030E+01 0.3998E+00 0.3485E+01
 0.0000E+00 0.9849E+00 0.6400E+02 0.4120E+01 0.4160E+00 0.3556E+01
 0.0000E+00 0.9841E+00 0.6500E+02 0.4209E+01 0.4323E+00 0.3628E+01
 0.0000E+00 0.9833E+00 0.6600E+02 0.4299E+01 0.4487E+00 0.3698E+01
 0.0000E+00 0.9825E+00 0.6700E+02 0.4387E+01 0.4652E+00 0.3768E+01
 0.0000E+00 0.9817E+00 0.6800E+02 0.4476E+01 0.4819E+00 0.3837E+01
 0.0000E+00 0.9808E+00 0.6900E+02 0.4564E+01 0.4986E+00 0.3906E+01
 0.0000E+00 0.9799E+00 0.7000E+02 0.4651E+01 0.5154E+00 0.3975E+01
 0.0000E+00 0.9790E+00 0.7100E+02 0.4738E+01 0.5323E+00 0.4042E+01
 0.0000E+00 0.9781E+00 0.7200E+02 0.4824E+01 0.5492E+00 0.4110E+01
 0.0000E+00 0.9772E+00 0.7300E+02 0.4910E+01 0.5662E+00 0.4176E+01
 0.0000E+00 0.9762E+00 0.7400E+02 0.4996E+01 0.5833E+00 0.4242E+01
 0.0000E+00 0.9752E+00 0.7500E+02 0.5081E+01 0.6004E+00 0.4308E+01
 0.0000E+00 0.9743E+00 0.7600E+02 0.5165E+01 0.6176E+00 0.4373E+01
 0.0000E+00 0.9733E+00 0.7700E+02 0.5249E+01 0.6348E+00 0.4437E+01
 0.0000E+00 0.9723E+00 0.7800E+02 0.5333E+01 0.6521E+00 0.4501E+01
```

```
C.....THIS PROGRAM (PLOTWQ2.FOR) IS USED TO CALCUATE AND PLOT
C.....THE HEAT REJECTION, COOLING CAPACITY AND WORK INPUT
C.....FOR CONSTANT FIELD CYCLE.
C.....PART OF INPUT FILE OF THIS PROGRAM IS THE OUTPUT OF " TOTEN.FOR ".
C....."DISSPLA" IS USED FOR PLOTTING.
      DIMENSION T(700),QH(700),QL(700),W(700),QHP(2),QLP(2),WP(2),TP(2)
      DIMENSION ST0(700),ST7(700)
      CHARACTER YTITLE*100,XTITLE*100,TITLE*100
      CHARACTER CYNAME*100,MATNAME*100
      INTEGER HFIELD,LFIELD,HT
       OPEN (UNIT=20,FILE='PLOTWQ2.DAT',STATUS='OLD')
       OPEN (UNIT=25,FILE='FOR99.DAT',STATUS='NEW')
        READ(20,*)HFIELD,LFIELD,HT
        READ(20,*)S1,S2,S3,S4,S5,S6
        READ(20,*)TITLE
        READ(20,*)XTITLE
        READ(20,*)YTITLE
        READ(20,*)CYNAME
        READ(20,*)MATNAME
        READ(20,*)RX0,RX1,RX2,RX3,RX4,RX5,RX6,RX7
        READ(20,*)RY0,RY1,RY2,RY3,RY4,RY5,RY6,RY7
        READ(20,*)TP(1),TP(2),QHP(1),QHP(2),QLP(1),QLP(2),WP(1),WP(2)
        READ(20,*)M
      DO 40 I=1,M
40      READ(20,*)T(M-I+1),ST0(M-I+1)
      DO 50 I=1,M
50      READ(20,*)T7,ST7(M-I+1)
        DSTH=ST0(1)-ST7(1)
        I=1
        SUM0=0.
        SUM7=0.
60      SUM0=SUM0+0.5*ABS((T(I+1)+T(I))*(ST0(I+1)-ST0(I)))
        SUM7=SUM7+0.5*ABS((T(I+1)+T(I))*(ST7(I+1)-ST7(I)))
        I=I+1
       IF(SUM7.GE.SUM0)THEN
         K=I
         SUML=0.
         SUM7F=SUM7
70       SUM7F=SUM7F-0.5*ABS((T(K)+T(K-1))*(ST7(K)-ST7(K-1)))
           IF(SUM7F.LE.SUM0)GO TO 80
         SUML=SUM7F
         K=K-1
         GO TO 70
80         IF(SUML.NE.0.)DELSUM=(SUM0-SUM7F)/(SUML-SUM7F)
           IF(SUML.EQ.0.)DELSUM=1.-(SUM7-SUM0)/(SUM7-SUM7L)
           QH(I)=HT*DSTH
           QL(I)=T(I)*(ST0(I)-(ST7(K-1)-ABS(ST7(K-1)-ST7(K))*DELSUM))
           W(I)=QH(I)-QL(I)
        END IF
       IF(SUM7.LT.SUM0)THEN
         QH(I)=HT*(DSTH-(SUM0-SUM7)/HT)
         QL(I)=T(I)*(ST0(I)-ST7(I))
         W(I)=QH(I)-QL(I)
        END IF
       IF(W(I).GT.0.)COP=QL(I)/W(I)
        WRITE(25,*)T(I),QL(I),COP
        IF(I.GE.M)GO TO 85
        SUM7L=SUM7
       GO TO 60
9     FORMAT(I6,10E10.3)
85     CALL COMPRS
```

```
CALL PAGE(11.,8.5)
CALL AREA2D(6.0,7.0)
CALL HEADIN(% REF(TITLE),100,1.5,1)
CALL XNAME(% REF(XTITLE),100)
CALL YNAME(% REF(YTITLE),100)
CALL INTAXS
CALL FRAME
CALL THKFRM(.01)
CALL GRAF(S1,S2,S3,S4,S5,S6)
CALL CURVE(T,QH,M,0)
CALL CURVE(TP,QHP,2,0)
CALL DASH
CALL CURVE(T,QL,M,0)
CALL CURVE(TP,QLP,2,0)
CALL DOT(T,W,M,0)
CALL CURVE(T,W,M,0)
CALL CURVE(TP,WP,2,0)
CALL RLMESS (% REF(MATNAME),100,RX0,RY0)
CALL RLMESS (% REF(CYNAME),100,RX1,RY1)
CALL RLMESS ('HIGH FIELD:  $',100,RX2,RY2)
CALL RLINT(HFIELD,'ABUT','ABUT')
CALL RLMESS ('LOW FIELD:   $',100,RX3,RY3)
CALL RLINT (LFIELD,'ABUT','ABUT')
CALL RLMESS ('HIGH TEMPERATURE:   $',100,RX4,RY4)
CALL RLINT (HT,'ABUT','ABUT')
CALL RLMESS ('HEAT REJECTION$',100,RX5,RY5)
CALL RLMESS ('COOLING CAPACITY$',100,RX6,RY6)
CALL RLMESS ('WORK INPUT$',100,RX7,RY7)
CALL ENDPL(0)
CALL DONEPL
STOP
END
```

```
C....PARTIAL LISTING OF DATA FILE "PLOTWQ2.DAT", INPUT FILE OF PLOTWQ2.FOR
7 0 320
0. 80. 320. 0. 20. 80.
' $'
'COOLING TEMPERATURE(K)$'
'ENERGY (Cal./g-mole)$'
'Cycle: Constant Field$'
'Material: Gd$'
10. 10. 10. 10. 10. 35. 35. 35.
78. 74. 70. 66. 35. 31. 27. 23.
10. 30. 31. 31. 27. 27. 23. 23.
541
 50.00000        2.827554
 50.50000        2.874455
 51.00000        2.921338
 51.50000        2.968196
 52.00000        3.015026
 52.50000        3.061821
 53.00000        3.108577
 53.50000        3.155288
 54.00000        3.201952
 54.50000        3.248562
 55.00000        3.295116
 55.50000        3.341609
 56.00000        3.388037
 56.50000        3.434397
 57.00000        3.480685
 57.50000        3.526898
 58.00000        3.573034
 58.50000        3.619089
 59.00000        3.665060
 59.50000        3.710945
 60.00000        3.756741
 60.50000        3.802445
 61.00000        3.848056
 61.50000        3.893571
 62.00000        3.938988
 62.50000        3.984305
 63.00000        4.029521
 63.50000        4.074633
 64.00000        4.119639
```

```
C.....THIS PROGRAM (PLOTWQ3.FOR) IS USED TO CALCULATE AND PLOT
C.....THE COOLING CAPACITY AND THE COP RATIOS OF A CONSTANT FILED CYCLE
C.....TO IDEAL REGENERATIVE CYCLE.
C.....PRAT OF INPUT FILE IS FROM THE OUTPUT FILES OF "PLOTWQ1.FOR" AND
C.....".PLOTWQ2.FOR".
C.....".DISSPLA" IS USED FOR PLOTTING.
      DIMENSION T(400),QL1(400),QL(400),QL2(400),COPP(2),QLP(2),TP(2)
      DIMENSION COP(400),COP1(400),COP2(400)
      CHARACTER YTITLE*100,XTITLE*100,TITLE*100
      CHARACTER CYNAME*100,MATNAME*100
      INTEGER HFIELD,LFIELD,HT
       OPEN (UNIT=20,FILE='PLOTWQ3.DAT',STATUS='OLD')
       OPEN (UNIT=25,FILE='FOR98.DAT',STATUS='NEW')
        READ(20,*)HFIELD,LFIELD,HT
        READ(20,*)S1,S2,S3,S4,S5,S6
        READ(20,*)TITLE
        READ(20,*)XTITLE
        READ(20,*)YTITLE
        READ(20,*)MATNAME
        READ(20,*)RX0,RX1,RX2,RX3,RX4,RX5,RX6,RX7
        READ(20,*)RY0,RY1,RY2,RY3,RY4,RY5,RY6,RY7
        READ(20,*)TP(1),TP(2),COPP(1),COPP(2),QLP(1),QLP(2)
        READ(20,*)M
      N=1
      DO 50 I=1,M
       K=M-I+1
       READ(20,*)T7,QL7,COP7
       IF(DMOD(DBLE(K),DBLE(2))+1 .EQ.2) THEN
         NK=(M/2 +1)-N+1
         QL2(NK)=QL7
         COP2(NK)=COP7
         WRITE(25,*)M,N,K,QL2(NK),COP2(NK),T7
          N = N+1
        END IF
50    CONTINUE
      READ(20,*)M
      DO 40 I=1,M
40      READ(20,*)T(I),QL1(I),COP1(I)
      DO 70 I=1,M
        QL(I)=QL2(I)/QL1(I)
        COP(I)=COP2(I)/COP1(I)
70    CONTINUE
9     FORMAT(I6,10E10.3)
       CALL COMPRS
       CALL PAGE(11.,8.5)
       CALL AREA2D(6.0,7.0)
       CALL HEADIN(% REF(TITLE),100,1.5,1)
       CALL XNAME(% REF(XTITLE),100)
       CALL YNAME(% REF(YTITLE),100)
       CALL INTAXS
       CALL FRAME
       CALL THKFRM(.01)
       CALL GRAF(S1,S2,S3,S4,S5,S6)
       CALL CURVE(T,COP,M,0)
       CALL CURVE(TP,COPP,2,0)
       CALL DASH
       CALL CURVE(T,QL,M,0)
       CALL CURVE(TP,QLP,2,0)
       CALL RLMESS (% REF(MATNAME),100,RX0,RY0)
       CALL RLMESS ('HIGH FIELD:  $',100,RX2,RY2)
       CALL RLINT(HFIELD,'ABUT','ABUT')
```

```
CALL RLMESS ('LOW FIELD:   $',100,RX3,RY3)
CALL RLINT (LFIELD,'ABUT','ABUT')
CALL RLMESS ('HIGH TEMPERATURE:   $',100,RX4,RY4)
CALL RLINT (HT,'ABUT','ABUT')
CALL RLMESS ('COP$',100,RX5,RY5)
CALL RLMESS ('CAP$',100,RX6,RY6)
CALL ENDPL(0)
CALL DONEPL
STOP
END
```

```
C....PARTIAL LISTING OF DATA FILE "PLOTWQ3.DAT", INPUT FILE OF PLOTWQ3.FOR
7 0 320
0. 80. 320. 0. 0.2 1.0
' $'
'COOLING TEMPERATURE(K)$'
'CONSTANT FIELD/IDEAL REGEN.$'
'Material: Gd$'
10. 10. 10. 10. 10. 35. 35. 35.
92. 92. 87. 825. 775. 725. 675. .625
10. 30. .725 .725 .675 .675
541
  320.0000        75.42664        318.9974
  319.5000        75.30878        639.0156
  319.0000        75.18910        316.5410
  318.5000        75.06821        209.4413
  318.0000        74.94552        155.7739
  317.5000        74.82283        123.9188
  317.0000        74.69835        102.5672
  316.5000        74.57207        87.26362
  316.0000        74.44463        75.80843
  315.5000        74.31660        66.95002
  315.0000        74.18742        59.86623
  314.5000        74.05585        54.02457
  314.0000        73.92315        49.16781
  313.5000        73.78989        45.08341
  313.0000        73.65549        41.58628
  312.5000        73.51935        38.54655
  312.0000        73.38089        35.87000
  311.5000        73.24250        33.53386
  311.0000        73.10239        31.45215
  310.5000        72.96059        29.58602
  310.0000        72.81708        27.90399
  309.5000        72.67366        26.39822
  309.0000        72.52796        25.02108
  308.5000        72.38059        23.76217
  308.0000        72.23156        22.60715
  307.5000        72.08263        21.55575
  307.0000        71.93146        20.58020
  306.5000        71.77865        19.67623
  306.0000        71.62420        18.83639
  305.5000        71.46929        18.05991
```

```
C
C       THIS PROGRAM IS MHSYS.FOR  IT IS FOR THE SIMULATION OF THE MH
C       SYSTEM TO BE BUILT.  THE EQUATIONS WERE TAKEN FROM BARCLAY
C       "THE THEORY  OF AN ACTIVE MAGYNETIC GENENERATIVE REFRIGERATOR".
C
        IMPLICIT REAL*8(A-H,O-Z)
        DIMENSION T(60,15),U(60,15),TE(60),DELTA(15),UD(60,15),
                  TD(60,15)
        DIMENSION TK(60,15),UK(60,15)
C
C       READ IN THE CONSTANTS
C
        OPEN (UNIT=20,FILE='MHSYS.DAT',STATUS='OLD',BLOCKSIZE=1800)
        OPEN (UNIT=6,FILE='MHSYS.OUT')
        READ(20,*)CF,CS,ALPHA,VF,RHOF,RHOS,TI
        READ(20,*)H,DKS,DI,DX,DT,M,N,DL
10      FORMAT(7F10.3)
11      FORMAT(2F10.2,F10.4,2F10.2,2I5,F10.2)
        PI=3.1415927D0
        A=PI*DI*DI/4.0D0/144.0D0
C
C       SETUP THE CONSTANTS FOR TEMPERATURE CALCULATION.
C
C       FLUID TEMPERATURE CONSTANTS
C
        C2 = VF*DT/3600.0D0/DX*12.0D0
        C3 = 2.0*H*DL*DT/3600.0D0/ALPHA/RHOF/CF/A
        C1 = 1.0D0 -C2-C3
C
C       GD CORE TEMPERATURE CONSTANTS
C
        C5 = 2.0D0*H*DL*DT/3600.0D0/(1.0D0-ALPHA)/RHOS/A/CS
        C6 = DKS*DT/3600.0D0/RHOS/CS/DX/DX*144.0D0
        C4 = 1.0D0-C5-2.0D0*C6
        WRITE(6,600)C1,C2,C3,C4,C5,C6
600     FORMAT(2X,6F9.4)
C
C       READ IN INITIAL FLUID AND GD TEMPERATURE, ASSUMED TO BE UNIFORM
C
        DO 21 J=1,N
        T(1,J)=TI
        U(1,J)=TI
        UK(1,J)=TI/1.8D0
        TK(1,J)=TI/1.8D0
21      CONTINUE
        DO 25 I=1,M
25      TE(I) = TI
        MM = 1
C
C       CALCULATE THE TEMPERATURE LIFT, OR FALL, OF GD CORE WHEN
C       MAGNETIZED, OR DE-MAGNETIZED
C
140     CONTINUE
        IF(MM .EQ.1)GO TO 160
        DO 170 J=1,N
        U(1,J) = UD(M,J)
        T(1,J) = TD(M,J)
        UK(1,J)=UD(M,J)/1.8D0
        TK(1,J)=TD(M,J)/1.8D0
170     CONTINUE
160     DO 40 J=1,N
```

```
      IF(UK(1,J) .GE. 200.0D0 .AND. UK(1,J) .LE. 250.0D0)
     * DELTA(J)=6.32D-4*UK(1,J)**2 - 2.146D-1*UK(1,J) + 21.83D0
      IF(UK(1,J) .GT. 250.0D0 .AND. UK(1,J) .LE. 293.0D0)DELTA(J)=
     * 2.5766D-3*UK(1,J)**2 - 1.2179445D0*UK(1,J) + 151.12708D0
      IF(UK(1,J) .GT. 293.0D0 .AND. UK(1,J) .LE. 350.0D0)DELTA(J)=
     * 1.380117D-3*UK(1,J)**2 - 1.0660117D0*UK(1,J) + 209.33D0
      DELTA(J)=DELTA(J)*1.8D0
      UK(1,J)=UK(1,J)*1.8D0
      IF(DMOD(DBLE(MM),DBLE(2))+1 .EQ. 2)U(1,J) = U(1,J) + DELTA(J)
      IF(DMOD(DBLE(MM),DBLE(2))+1 .NE. 2)U(1,J) = U(1,J) - DELTA(J)
      WRITE(6,500)J,DELTA(J),UK(1,J),U(1,J)
500   FORMAT(2X,I3,3F10.2)
40    CONTINUE
C
C     START MARCHING OF U & T IN TIME "t" AND ALONG GD CORE "X"
C
      DO 45 I=1,M-1
      DO 50 J=1,N
      IF(J.NE.1)GO TO 52
      T(I+1,J) = C1*T(I,J)+C2*TE(I)+C3*U(I,J)
      U(I+1,J) = C4*U(I,J)+C5*T(I,J)+C6*2.0D0*U(I,J+1)
      IF(J.EQ.1)GO TO 50
52    T(I+1,J) = C1*T(I,J)+C2*T(I,J-1)+C3*U(I,J)
      IF(J .EQ. N) GO TO 54
      U(I+1,J) =C4*U(I,J) + C5*T(I,J) + C6*(U(I,J+1) + U(I,J-1))
      GO TO 50
54    U(I+1,J) =C4*U(I,J) + C5*T(I,J) + C6*2.0D0*U(I,J-1)
50    CONTINUE
C      WRITE (6,90) MM,I,J-1,U(I,J-1),T(I,J-1),DELTA(J-1)
100   CONTINUE
90    FORMAT(2X,3I3,2X,3F10.3)
C56    IF(U(I+1,J) .GT. 630.0D0 .OR. U(I+1,J) .LT.360.0D0)GO TO 125
45    CONTINUE
      DO 750 J=1,N
750   WRITE(6,760)M,MM,J,U(M,J),T(M,J)
760   FORMAT(2X,3I3,2F10.2)
C
C     STORE FLUID TEMPERATURE OUT OF GD CORE
C
      DO 60 I = 1,M
      LL=DBLE(M)-DBLE(I)+DBLE(1)
60    TE(LL) = T(I,N)
      DO 770 I = 1,M,10
770   WRITE(6,660)I,TE(I),T(I,N)
660   FORMAT(10X,I3,2F10.3)
C
C
      MM=MM+1
      IF(MM .GT. 51)GO TO 130
C
C     START REVERSING THE FLOW & CHANGE THE MAGNETIOC PROCESS
C
      DO 70 J=1,N
C
C     ADD THE NEXT FOUR LINES TO ASSUME THE EVEN OUT OF FLUID AND
C     MAGNETIC CORE TEMPERATURE DURING THE GD CORE "STOP" PERIOD
C
      T(M,J)=(ALPHA*RHOF*CF*T(M,J)+(1.0D0-ALPHA)*RHOS*CS*U(M,J))
     ./(ALPHA*RHOF*CF+(1.0D0-ALPHA)*RHOS*CS)
      U(M,J)=T(M,J)
      TD(M,N-J+1) = T(M,J)
```

```
        UD(M,N-J+1) = U(M,J)
70      CONTINUE
        I=1
        GO TO 140
C125     WRITE(6,150)
C150     FORMAT(' U IS EITHER LARGER THAN 630.0, OR SMALLER THAN 360.0')
130     STOP
        END
```

```
C....DATA FILE "MHSYS.DAT", INPUT FILE OF MHSYS.FOR.............
0.24  0.055   0.700 1000.000  0.075  491.000   480.000  540.000
500.0  5.20  20.000  0.8  0.0150   60  6  1.00  530. 2.0
 0. 0.785 3.14 440.0 20. 580. 10 50
```

DISTRIBUTION FOR REPORT ORNL/TM-11608

1. B. Buchanan, Computer Science Department, University of Pittsburgh, 206 Mineral Industries Building, Pittsburgh, PA 15260
2. J. J. Cuttica, Vice President, End Use Research and Development, Gas Research Institute, 8600 W. Bryn Mawr Avenue, Chicago, Il 60631
3. A. Hirsch, President, Dynamac Corporation, The Dynamac Building, 11140 Rockville Pike, Rockville, MD 20852
4. D. E. Morrison, 333 Oxford Road, East Lansing, MI 48823
5. M. Williams, Professor, Department of Economics, Northern Illinois University, DeKalb, IL 60115

6-7. Office of Scientific and Technical Information, P.O. Box 62, Oak Ridge, TN 37831

8-18. F. C. Chen

19. G. L. Chen
20. M. S. Lubell
21. J. W. Lue

22-32. V. C. Mei

33. R. W. Murphy
34. L. Boch, JPL
35. R. S. Carlsmith
36. G. E. Courville
37. M. E. Gunn, DOE
38. B. Johnson, PNL
39. M. A. Kuliasha
40. D. E. Reichle
41. R. B. Shelton
42. S. Sohel, INEL
43. A. Thomas, ANL
44. Assistant Manager Energy Research & Development, DOE/ORO
45. ORNL Patent Office
46. Central Research Library
47. Document Reference Section

48-50. Laboratory Records Department

51. Laboratory Records Department - RC